

Keldysh Green's function approach to coherence in a non-equilibrium steady state: connecting Bose-Einstein condensation and lasing

Jonathan Keeling, Marzena H. Szymańska and Peter B. Littlewood

Abstract:

Solid state quantum condensates often differ from previous examples of condensates (such as Helium, ultra-cold atomic gases, and superconductors) in that the quasiparticles condensing have relatively short lifetimes, and so as for lasers, external pumping is required to maintain a steady state. On the other hand, compared to lasers, the quasiparticles are generally more strongly interacting, and therefore better able to thermalise. This leads to questions of how to describe such non-equilibrium condensates, and their relation to equilibrium condensates and lasers. This chapter discusses in detail how the non-equilibrium Green's function approach can be applied to the description of such a non-equilibrium condensate, in particular, a system of microcavity polaritons, driven out of equilibrium by coupling to multiple baths. By considering the steady states, and fluctuations about them, it is possible to provide a description that relates both to equilibrium condensation and to lasing, while at the same time, making clear the differences from simple lasers.

Jonathan Keeling
Cavendish Laboratory, University of Cambridge, email: jmjk2@cam.ac.uk
Marzena H. Szymańska
Department of Physics, University of Warwick, email: M.H.Szymanska@warwick.ac.uk
also at London Centre for Nanotechnology
Peter Littlewood
Cavendish Laboratory, University of Cambridge, email: pbl21@cam.ac.uk

Bose-Einstein condensation (BEC), the equilibrium phase transition of weakly interacting bosons, was realised over ten years ago in ultra-cold atomic gases. After long and strenuous efforts to observe this state in solids, BEC of polaritons[1] and of magnons[2] were reported. These reports followed observations of related effects for excitons in quantum Hall bilayers[3], spin triplet states in magnetic insulators[4] and excitons in coupled quantum wells[5–7]. Solid-state condensates depart from the archetypal BEC in several ways. Most importantly they live for short times and rely on external pumping. Indeed, it was the decay, and consequent lack of equilibrium, which for a long time presented the obstacle the realisation of solid-state BEC. Even if one can accelerate thermalisation, the decay, and the consequent flux of particles, remains a more important effect in solid state than it generally does in cold atomic gases, or in other quantum condensates such as superfluid Helium.

When considering whether such a system may be treated as equilibrium or not, there are several distinct characterisations of the degree to which the system is non-equilibrium. The most obvious compares particle lifetime to the time required for collisions to thermalise the system, determining the extent to which a thermal distribution may arise. The timescale for establishing a thermal distribution within one part of the system can however be quite different to that for establishing either thermal or chemical equilibrium between different parts of the system. Another characterisation of whether non-equilibrium physics is relevant arises from comparing the linewidth due to finite particle lifetime to the temperature of the system, thus determining whether lifetime or temperature effects dominate coherence properties. Table 0.1 summarises the typical timescales and energy scales connected with different examples of metastable quantum condensates. It is clear that the ratio of thermalisation time to the particle lifetime is generally somewhat larger for solid-state condensates than it is for cold atomic gases. If one instead compares the ratio of the linewidth due to decay to the characteristic temperature, polaritons stand out as having a decay linewidth of the same order of magnitude as their temperature. As such, polaritons are good systems in which to study effects of finite lifetime on coherence properties.

	Lifetime	Thermalisation	Linewidth	Temperature	
Atoms[8]	10s	10ms	2.5×10^{-13} meV	10^{-8} K	10^{-9} meV
Excitons[9]	50ns	0.2ns	5×10^{-5} meV	1K	0.1meV
Polaritons[10]	5ps	0.5ps	0.5meV	20K	2meV
Magnons[2]	1μ s	100ns	2.5×10^{-6} meV	300K	30meV

Table 0.1: Characteristic timescales and energies for: particle lifetimes, times to establish a thermal distribution, linewidth due to finite lifetime, and characteristic temperatures for various candidate condensates. Comparison of the first two describes how thermal the distribution will be; comparison of the later two determine the effect of finite lifetime on coherence properties.

Because, as we will discuss further below, polariton condensates provide such a clear illustration of the properties of non-equilibrium condensation, we will focus on them in particular. Microcavity polaritons are the quasiparticles which result from strong coupling between photons confined in a semiconductor microcavity, and excitons in a quantum well. By changing the detuning between the excitons and photons, and by changing the strength of an external pump that injects polaritons, one can modify the polariton mass, density and the effect of interactions between polaritons. A more detailed introduction to microcavity polaritons and semiconductor microcavities can be found in several review articles and books [11–17]

The intrinsic non-equilibrium and dissipative nature of solid-state condensates, especially of polaritons, brings connections to other systems exhibiting macroscopic coherence, i.e lasers. With the realisation of more complex, interaction dominated lasers, such as random lasers (see

e.g. Refs. [18, 19]) or atom lasers (e.g. Refs.[20–22]), this connection is particularly pronounced. Compared to simple lasers, polaritons are however more strongly interacting, and therefore much better able to thermalise than are photons, and so in many ways solid-state condensates can be viewed as being somewhere in between an equilibrium BEC and a laser. At the same time, at large temperatures and/or in the presence of large decoherence mechanisms and large pumping the same microcavity system supports a simple lasing action. In this context, microcavity polaritons provide particularly excellent playground for studying coherence in a dissipative environment, and the differences and similarities between condensates and lasers. Clearly, an approach which takes into account the non-equilibrium and dissipative nature of this new state of matter, as well as strong interactions, multimode-structure, low dimensionality and finite size is necessary.

This chapter will discuss a theoretical approach to modelling quantum condensates that are driven out of equilibrium by a flow of particles through the system. We therefore consider coupling the system to baths, which can transfer energy as well as particles to and from the system. With such baths, we find that the behaviour of a simple laser can be recovered in the limit of high temperature baths. A different scenario of how decoherence affects condensation can be found if one considers static disorder — i.e. allowing scattering, but with no transfer of energy to or from the system. Such a problem [23, 24] is closely related to the Abrikosov-Gorkov approach to disordered superconductors[25]. As in the case of superconductors, one finds a distinction between “pair-breaking” and “non-pair-breaking” disorder (respectively magnetic and non-magnetic impurities in the superconducting case). As expected from Anderson’s theorem[26], the coherence associated with the condensate leads to a gap in the exciton density of states, which makes the condensate robust to non-pair-breaking disorder. With pair-breaking disorder, decoherence eventually destroys the gap and finally the condensate, but for small amounts of decoherence, the gap protects the condensate. A similar scenario also exists in the ultra high density limit, where excitons are destroyed by screening, leading to an electron-hole plasma phase[27], which can nonetheless support lasing. While we focus in this chapter instead on the effects of particle flux, and baths that can transfer energy, these other results illustrate that there are a variety of ways in which decoherence can either suppress or modify the properties of a condensate. In principle one can have both a crossover from a polariton condensate to a regular laser (weak coupling but still excitonic gain medium, as discussed here), and a crossover to a particle-hole laser (weak coupling, electron-hole plasma, if screening is strong).

The approach to modelling the condensate with a flux of particles presented in this chapter is based on work by the authors in Refs.[28, 29]. While in those works, the results were derived and presented making use of the non-equilibrium path integral approach[30], both the results and their theoretical basis can be understood without this technical background, by considering the diagrammatic approach to calculating non-equilibrium Green’s functions [31–33]. The particular aim of this chapter is therefore to review some of these results, illustrating in some detail how a steady state non-equilibrium system which develops spontaneous coherence, can be treated in the non-equilibrium diagrammatic formalism. At the same time, this approach will provide a natural language to highlight the way this system relates both to equilibrium condensates and to lasers, and to understand the ingredients that makes it differ from these limits.

There are a number of other known approaches to describing systems driven out of equilibrium by coupling to multiple baths. Those that have been applied to microcavity polaritons include: quantum kinetic equations[34–41], Heisenberg-Langevin equations[42], stochastic methods for density matrix evolution (i.e. truncated Wigner approximation)[43, 44]; as well as mean-field approaches, considering the complex Gross-Pitaevskii equation, in some cases including also coupling to reservoirs or thermal baths [45–47]. While this chapter does not intend to review the merits of each of these approaches, it is worth noting that in general, these approaches are all connected. The connections between many of them can simply be seen by looking at

their relation to the non-equilibrium diagrammatic approach. As discussed in [33, 48], the quantum Boltzmann equation can be derived as an equation for the distribution function that appears in the Keldysh Green's function, along with a Wigner transformation from $F(t, r, t', r')$ to $F(T, R, \omega, p)$. It will become clear from the discussion in Sec. 3, that there is a close analogy between the Keldysh Green's functions and the Heisenberg-Langevin equations, with the bath Green's functions describing the same physics as the correlation functions of the bath noise operators in the Heisenberg-Langevin approach. There also exists a connection between the approach described here and density matrix evolution. The single particle density matrix is given by $\langle \psi^\dagger(r, t) \psi(r', t) \rangle$, and thus corresponds to an appropriate combination of equal time Green's functions. The density matrix naturally gives single time expectations of appropriate observables, it is also possible to derive two-time correlations from the time evolution of the density matrix, by means of the quantum regression theorem[49]. The quantum regression theorem however relies on making an additional Markov approximation regarding the bath occupations, as well as a Markov approximation for the bath density of states[50]. The Keldysh Green's function approach does not require this additional Markov approximation; and in fact Sec. 4 will show how making this further approximation restricts the conditions for condensation to occur.

In order to illustrate the application of the non-equilibrium technique, we consider a specific model of microcavity polaritons, starting from disorder localised excitons strongly coupled to cavity photons[51–53]. In this model, interactions between excitons are included by treating the excitons as hard-core bosons, allowing one exciton, but no more, to occupy a given disorder localised state. For the discussion presented here, using this model provides a number of technical advantages: it connects closely to the idea of gain from two-level systems that is typically used in models of simple lasers[49], making the comparison to lasing straightforward; and it automatically includes nonlinearity of the excitons, allowing this nonlinearity to be described by the properties of the exciton representation, rather than requiring higher order diagrammatic corrections. In addition, in an equilibrium situation, the mean-field theory of this model is known to give a reasonable description of the critical temperature, except at very low densities where fluctuation corrections become important[52].

This chapter is organised as follows; section 1 introduces the model Hamiltonian, and its coupling to baths. Section 2 then describes the approach we will take to modelling this system, reviewing some standard results of the non-equilibrium diagrammatic technique that will be used later, and discussing the mean-field approach we use to find the steady state. In order to evaluate this mean-field condition, it is necessary to determine the effects of the baths on the system, by calculating particular self energy diagrams, these self energies are presented in section 3. Section 4 then discusses the mean-field theory, considering how it can recover both equilibrium results in one limit, as well as the description of a simple laser in another limit. Section 5 discusses fluctuations about the steady state, analysing stability, and further illuminating the connection to (and distinctions from) a simple laser; section 6 then provides a more qualitative discussion of the fluctuations of the condensed system, focusing in particular on the combined effect of finite size and finite lifetimes.

1 Polariton system Hamiltonian, and coupling to baths

As explained above, we consider a model of excitons as hard core bosons coupled to propagating photons. To write the Hamiltonian for hard-core bosons, it is convenient to introduce fermionic operators b_i^\dagger, a_i^\dagger , such that the two fermionic states represent the presence or absence of an exciton on a given site, hence the operator $b_i^\dagger a_i$ is the exciton creation operator. With this

notation, the system is described by:

$$H_{\text{sys}} = \sum_i \epsilon_i (b_i^\dagger b_i - a_i^\dagger a_i) + \sum_k \omega_k \psi_k^\dagger \psi_k + \sum_{i,k} g_i (\psi_k^\dagger a_i^\dagger b_i + \text{H.c.}), \quad (1)$$

where ϵ_i is the energy of a localised exciton state, g_i is the exciton-photon coupling strength, and $\omega_k = \omega_0 + k^2/2m_{\text{phot}}$ is the dispersion of cavity photons. As sketched in Fig. 0.1, this can then be driven out of equilibrium by coupling to two baths, so the the system evolves under the full Hamiltonian $H = H_{\text{sys}} + H_{\text{sys,bath}} + H_{\text{bath}}$. It will be useful later on to divide the coupling to baths into coupling to the pumping bath, and coupling to the decay bath $H_{\text{sys,bath}} = H_{\text{sys,bath}}^{\text{pump}} + H_{\text{sys,bath}}^{\text{decay}}$ where the forms of the coupling to the pumping and decay baths are:

$$H_{\text{sys,bath}}^{\text{pump}} = \sum_{n,i} \Gamma_{n,i} (a_i^\dagger A_n + b_i^\dagger B_n + \text{H.c.}), \quad H_{\text{sys,bath}}^{\text{decay}} = \sum_{p,k} \zeta_{p,k} (\psi_k^\dagger \Psi_p + \text{H.c.}). \quad (2)$$

Here $\Gamma_{n,i}$ is the coupling to a pumping bath, described by the fermionic operators B_n^\dagger, A_n^\dagger , and $\zeta_{p,k}$ is the coupling to decay bath, describing bulk photon modes Ψ_p^\dagger . The bath Hamiltonian is taken to have the simple quadratic form:

$$H_{\text{bath}} = \sum_n \nu_n^\Gamma (B_n^\dagger B_n - A_n^\dagger A_n) + \sum_p \omega_p^\zeta \Psi_p^\dagger \Psi_p \quad (3)$$

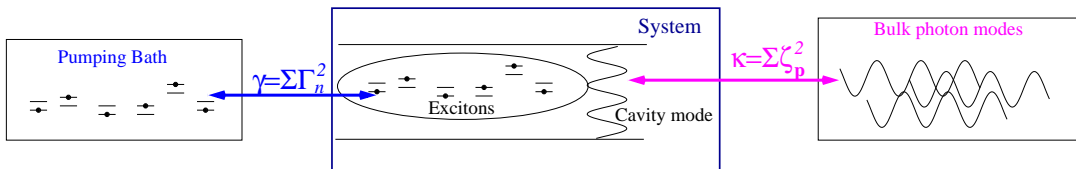


Figure 0.1: Cartoon of system, consisting of photons strongly coupled to excitons, and external baths, describing pumping and decay. Adapted from Ref.[29].

Describing the pumping reservoir and photon decay as baths means that we assume these both contain many modes (i.e. are much larger than the system), and thermalise rapidly compared to the interaction with the system. These assumptions mean that one may impose a particular distribution function on the bath modes, and then determine what distribution the system adopts; we will take a thermal distribution for the pumping bath, specified by a bath temperature and chemical potential, and we will assume the bulk photon modes are unoccupied. Note that we do not explicitly introduce any system chemical potential, as the density of the system will be fixed by the balance of pumping and decay, however a natural definition of the system chemical potential will arise later.

2 Modelling the non-equilibrium system

The Keldysh non-equilibrium diagrammatic technique[31] is an approach well suited to dealing with the kind of non-equilibrium steady state which we consider here. Section 2 briefly summarises the concepts that will be important in the remainder of this chapter; for a more complete introduction, see for example Refs. [31–33]. Within this diagrammatic approach, we will then determine the possible steady states of the system by a mean-field approach, introduced in section 2.

Non-equilibrium diagram approach

In order to determine both the spectrum (i.e. the ground and excited states, taking into account interactions and coupling to baths), and the non-equilibrium occupation of this spectrum, it is necessary to calculate two linearly independent Green's functions; it is convenient to make these the retarded and Keldysh Green's functions:

$$D^R(t, r) = -i\theta(t) \langle [\psi(t, r), \psi^\dagger(0, 0)]_- \rangle, \quad D^K(t, r) = -i \langle [\psi(t, r), \psi^\dagger(0, 0)]_+ \rangle. \quad (4)$$

Here, $[\psi, \psi^\dagger]_{\mp}$ indicates the commutator (anti-commutator) of ψ and ψ^\dagger . These Green's functions can be written as time-ordered products of fields by introducing the Keldysh contour, shown in Fig. 0.2. Each point on this contour is labelled by $(t, \{f, b\})$, where the f, b label whether it is

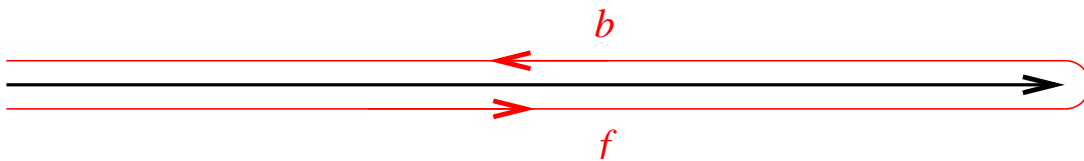


Figure 0.2: Keldysh closed-time-path contour, which can generate multiple orderings of fields

on the forward or backward branch. We then introduce the contour time ordering T_c , such that fields on the backward contour are always later than those on the forward contour, and that pairs of fields on the backward contour should appear in reverse order. By then introducing symmetric and anti-symmetric combinations of these fields $\psi_{\pm} = [\psi(t, f) \pm \psi(t, b)] / \sqrt{2}$, one may write the Green's function:

$$D = \begin{pmatrix} D^K & D^R \\ D^A & 0 \end{pmatrix} = -i \left\langle T_c \begin{pmatrix} \psi_+(t, r) \\ \psi_-(t, r) \end{pmatrix} \left(\psi_+^\dagger(0, f), \psi_-^\dagger(0, b) \right) \right\rangle. \quad (5)$$

Here, D^A refers to the advanced Green's function, which is the Hermitian conjugate of the retarded Green's function.

Given the above time-ordered products, one may use standard methods[54, 55] to write a diagrammatic expansion, by writing the Heisenberg picture fields in terms of the interaction picture fields $\tilde{\psi}(t)$:

$$\psi(t) = U^{-1}(t)\tilde{\psi}(t)U(t), \quad \tilde{\psi}(t) = e^{iH_0 t}\psi e^{-iH_0 t}, \quad (6)$$

where $H = H_0 + H_{\text{int}}$, and H_0 is “free”, meaning that it is simple to write expectations of products of fields evolving according to H_0 . By formally solving the equation for $U(t)$, one may then write the Green's functions in the following form:

$$D = -i \left\langle T_c \left[\begin{pmatrix} \tilde{\psi}_+(t, r) \\ \tilde{\psi}_-(t, r) \end{pmatrix} \left(\tilde{\psi}_+^\dagger(0, 0), \tilde{\psi}_-^\dagger(0, 0) \right) U \right] \right\rangle \quad (7)$$

$$U = \exp \left[-i \int_C \tilde{H}_{\text{int}}(t) dt \right] = \exp \left[-i \int_{-\infty}^{\infty} \left(\tilde{H}_{\text{int}}(t, f) - \tilde{H}_{\text{int}}(t, b) \right) dt \right]. \quad (8)$$

The diagrammatic expansion then follows by expanding the exponential, which produces vertices coupling free fields, and connecting these vertices by lines representing the Green's functions of the free fields. Compared to other diagrammatic expansions, the only extra complication is to keep track of the \pm labels on the fields, both in the matrix structure of Keldysh/retarded/advanced Green's functions, and in the form of U .

In the following, we will frequently make use of the Dyson equation[33, 54, 55], $D^{-1} = D_0^{-1} - \Sigma$, and so it is useful to record the free inverse Green's function. The inverse Green's function has the structure:

$$D^{-1} = \left[\begin{pmatrix} D^K & D^R \\ D^A & 0 \end{pmatrix} \right]^{-1} = \begin{pmatrix} 0 & [D^A]^{-1} \\ [D^R]^{-1} & [D^{-1}]^K \end{pmatrix}, \quad (9)$$

where $[D^{-1}]^K = -[D^R]^{-1} D^K [D^A]^{-1}$. Using the results for a free field, one has

$$[D_0^R]^{-1} = \omega - \omega_k + i\eta, \quad [D_0^{-1}]^K = (2i\eta)(2n_B(\omega) + 1), \quad (10)$$

where η is infinitesimal. All of the results noted above assume bosonic fields; the results for fermionic fields are similar, but commutators and anti-commutators are interchanged in the definitions of Keldysh and retarded Green's functions.

For our particular model of microcavity polaritons, the division of the full Hamiltonian into H_0 and H_{int} will be to take:

$$H_0 = \sum_i \epsilon_i (b_i^\dagger b_i - a_i^\dagger a_i) + \sum_k \omega_k \psi_k^\dagger \psi_k + \sum_i g_i \psi_0 \left(e^{i\mu_S t} a_i^\dagger b_i + e^{-i\mu_S t} b_i^\dagger a_i \right) + H_{\text{bath}} \quad (11)$$

where ψ_0 is a mean-field coherent photon field, as discussed in the next section. This means that H_{int} will contain the system-bath interactions, as well as the interaction between the two-level systems and incoherent photon fluctuations. In the following we will however generally focus on one part of H_{int} at a time.

Mean-field condition for coherent state

For a system coupled to multiple baths, the mean-field theory can no longer be thought of as minimising free energy, but rather as a stable self consistent steady state. For a condensed solution, one looks for a steady state of the form $\langle \psi_k \rangle = \psi_0 \exp(-i\mu_S t) \delta_{k,0} = \psi_0(t) \delta_{k,0}$, where μ_S is introduced here merely as part of the steady state ansatz, but it will be seen to play a role analogous to the equilibrium chemical potential. To be a self-consistent solution, this ansatz must satisfy the Heisenberg equation: $\langle i\partial_t \psi \rangle = \langle [\psi, H] \rangle$, and so:

$$\mu_S \psi_0(t) = \omega_0 \psi_0(t) + \sum_i g_i \langle a_i^\dagger(t) b_i(t) \rangle + \sum_p \zeta_{p,0} \langle \Psi_p(t) \rangle. \quad (12)$$

The expression $\langle a_i^\dagger(t) b_i(t) \rangle$ describes the polarisation of the two-level systems, and can be written in terms of the Keldysh Green's function, as:

$$\langle a_i^\dagger(t) b_i(t) \rangle = \frac{1}{2} \left\langle \left[b_i(t), a_i^\dagger(t) \right]_- \right\rangle = \frac{i}{2} G_{a_i^\dagger b_i}^K(t, t) = \frac{i}{2} \int \frac{d\nu}{2\pi} G_{a_i^\dagger b_i}^K(\nu). \quad (13)$$

As well as this self-consistency condition to determine the coherent field amplitude and the effective system chemical potential μ_S , the mean-field approach can also be used to give an estimate of the polariton density. This density will be used later in producing the phase diagram of the polariton condensate. The mean-field estimate of the total density is given by the combination of the photon density $|\psi_0|^2$, and the fermion density $(i/2)\text{Tr}[G_{b_i^\dagger b_i}^K - G_{a_i^\dagger a_i}^K]$.

3 Effects of baths on system correlation functions

In the above, we found that the mean-field condition could be written in terms of the two-level system Green's function, and the expectation of the decay bath fields. In this section we will discuss in detail the treatment of the baths and their effect on system's correlation functions, which will then determine the conditions under which a condensed solution may exist. Most of the effort, in Sec. 3, will be dedicated to finding $G_{a_i^\dagger b_i}^K(\nu)$ including the effects of pumping. Before doing this, section 3 will address the simpler problem of how $\langle \Psi_p(t) \rangle$ can be related to the decay bath Green's function and thus evaluated.

Decay bath and $\langle \Psi_p \rangle$

To calculate $\langle \Psi_p(t) \rangle$ in terms of non-equilibrium Green's functions, one may first use the interaction picture, in terms of the system-bath coupling, to write $\Psi_p(t) = U^{-1}(t)\tilde{\Psi}_p(t)U(t)$. Here, $U(t)$ is the time-ordered exponential as in Eq. (6):

$$U(t) = T \exp \left[-i \int_{-\infty}^t dt' \tilde{H}_{\text{sys,bath}}^{\text{decay}}(t') \right]. \quad (14)$$

Then, consider inserting a factor:

$$1 = T \exp \left[i \int_t^\infty dt' \tilde{H}_{\text{sys,bath}}^{\text{decay}}(t') \right] \cdot T \exp \left[-i \int_t^\infty dt' \tilde{H}_{\text{sys,bath}}^{\text{decay}}(t') \right], \quad (15)$$

either before or after $\tilde{\Psi}_p(t)$. The resulting expression implies that one has:

$$\langle \Psi_p(t) \rangle = \langle T_C[\tilde{\Psi}_p(t, f)U] \rangle = \langle T_C[\tilde{\Psi}_p(t, b)U] \rangle = \frac{1}{\sqrt{2}} \langle T_C[\tilde{\Psi}_{p,+}(t)U] \rangle, \quad (16)$$

where the last equality has made use of the fact that if the expectation of $\tilde{\Psi}(t, f)$ and $\tilde{\Psi}(t, b)$ match, then the expectation of $\tilde{\Psi}_-(t)$ must vanish. We are interested in particular in the value of this expectation $\langle \Psi_p \rangle$ when we consider the system in the mean-field approximation. In this case the system bath interaction term is given by:

$$\int_C dt \tilde{H}_{\text{sys,bath}}^{\text{decay}}(t) = \int_{-\infty}^\infty dt \sum_p \zeta_{p,0} \sqrt{2} [\tilde{\Psi}_{p,-}^\dagger(t) \psi_0(t) + \psi_0^*(t) \tilde{\Psi}_{p,-}(t)]. \quad (17)$$

With vertices given by this interaction, the set of diagrams involved in evaluating Eq. (16) is particularly simple: the only possible connected diagram is one with a single bath Green's function connecting the source term in $H_{\text{sys,bath}}$ to the field $\tilde{\Psi}_+$ that we want to measure. As such, the sum appearing in Eq. (12) can be written as:

$$\sum_p \zeta_{p,0} \langle \Psi_p(t) \rangle = \sum_p \zeta_{p,0}^2 \int dt' D_{\tilde{\Psi}_p^\dagger \Psi_p}^R(t, t') \psi_0(t'). \quad (18)$$

The simple form this equation takes is also the form one would find by making the Born approximation; i.e. assuming that $\zeta_{p,0}$ is small, so that terms like $\sum_p \zeta_{p,0}^2$ should be kept, and neglecting terms involving any higher power of $\zeta_{p,0}$. However, in the current case, because of the linearity of the coupling, no other connected diagrams exist, so no assumption of smallness is required in order to neglect higher order terms.

For a free bath, one may write $\tilde{\Psi}_p(t) = e^{-i\omega_p^\dagger t} \Psi_p$, and so the bath Green's function is given by $D_{\tilde{\Psi}_p^\dagger \Psi_p}^R(t, t') = -i\theta(t-t')e^{-i\omega_p^\dagger(t-t')}$. Taking a Markovian approximation for the bath density

of states and coupling [i.e assuming that the product of the bath density of states $N^\zeta(\omega)$ and the square of the system–bath coupling $\zeta_{p,0}$ are constant: $\pi\zeta_{p,0}^2N^\zeta(\omega) = \kappa$] then gives:

$$\sum_p \zeta_{p,0}^2 e^{-i\omega_p^S(t-t')} = 2\kappa\delta(t-t'). \quad (19)$$

Putting this all together, the net effect of the decay bath on the self-consistency equation is just to add a decay term, so the result may be written as:

$$(\omega_0 - \mu_S - i\kappa)\psi_0 e^{-i\mu_S t} = - \sum_i \frac{ig_i}{2} \int \frac{d\nu}{2\pi} G_{a_i^\dagger b_i}^K(\nu). \quad (20)$$

Pumping bath and $G_{a^\dagger b}^K$

The remaining task is to find the matrix of fermionic Green's functions in the four by four space resulting from the a, b fermionic fields and the \pm space associated with the closed-time-path contour. As above, we will take the interaction Hamiltonian to be the coupling between the system and the bath. This leaves the free fermion Hamiltonian:

$$H_0^{\text{TLS}} = \sum_i \epsilon_i (b_i^\dagger b_i - a_i^\dagger a_i) + \sum_i g_i \psi_0 \left(e^{i\mu_S t} a_i^\dagger b_i + e^{-i\mu_S t} b_i^\dagger a_i \right). \quad (21)$$

It is possible to diagonalise this Hamiltonian by a unitary transformation, and thereby write the appropriate free Green's function, however it is first necessary to remove the time dependence introduced by the form of the ansatz for the coherent field. This can be achieved by a gauge transformation:

$$H \rightarrow H - \frac{\mu_S}{2} \left[\sum_i (b_i^\dagger b_i - a_i^\dagger a_i) + \sum_n (B_n^\dagger B_n - A_n^\dagger A_n) \right]. \quad (22)$$

such that $b \rightarrow be^{-i\mu_S t/2}, a \rightarrow ae^{i\mu_S t/2}$, which removes the time dependence of the mean-field photon to fermion coupling. The gauge transformation for the bath modes that also appears in Eq. (22) is necessary to ensure no time dependence is introduced into the system-bath coupling terms. The net result is to replace $\epsilon_i \rightarrow \tilde{\epsilon}_i = \epsilon_i - \mu_S/2$ in H_0^{TLS} , and to shift the bath Green's function in frequency by $\pm\mu_S/2$.

After the above transformation, the Hamiltonian can be diagonalised by the unitary transformation:

$$\begin{pmatrix} b_i \\ a_i \end{pmatrix} = \begin{pmatrix} \cos(\theta_i) & \sin(\theta_i) \\ -\sin(\theta_i) & \cos(\theta_i) \end{pmatrix} \begin{pmatrix} \beta_i \\ \alpha_i \end{pmatrix}, \quad (23)$$

after which the free Hamiltonian takes the form $H_0^{\text{TLS}} = \sum_i E_i (\beta_i^\dagger \beta_i - \alpha_i^\dagger \alpha_i)$, where $\tan(2\theta_i) = -g_i \psi_0 / \tilde{\epsilon}_i$ and $E_i^2 = \tilde{\epsilon}_i^2 + g_i^2 \psi_0^2$. Since the Hamiltonian is diagonal in the β, α basis, the retarded Green's functions in that basis are just $[\nu \mp E_i + i\eta]^{-1}$ (where η is infinitesimal), and so the retarded Green's functions in the b, a basis can be written as:

$$\begin{aligned} G_0^R(\nu) &= \begin{pmatrix} \cos \theta_i & \sin \theta_i \\ -\sin \theta_i & \cos \theta_i \end{pmatrix} \begin{pmatrix} [\nu - E_i + i\eta]^{-1} & 0 \\ 0 & [\nu + E_i + i\eta]^{-1} \end{pmatrix} \begin{pmatrix} \cos \theta_i & -\sin \theta_i \\ \sin \theta_i & \cos \theta_i \end{pmatrix} \\ &= \frac{1}{(\nu + i\eta)^2 - E_i^2} \begin{pmatrix} \nu + \tilde{\epsilon}_i + i\eta & g_i \psi_0 \\ g_i \psi_0 & \nu - \tilde{\epsilon}_i + i\eta \end{pmatrix} \end{aligned} \quad (24)$$

$$[G_0^R]^{-1} = \begin{pmatrix} \nu - \tilde{\epsilon}_i + i\eta & -g_i \psi_0 \\ -g_i \psi_0 & \nu + \tilde{\epsilon}_i + i\eta \end{pmatrix}. \quad (25)$$

Clearly, if ψ_0 is zero then the a, b fields decouple as expected. However for non-zero ψ_0 , the Keldysh Green's functions of the two fields get mixed, so that their occupation is set by a balance of the pumping and the effects of the coherent photon field.

To complete our analysis, we should invert the above matrix to find the Keldysh block, and the $a^\dagger b$ component of that block. Using the Keldysh block structure of Eq. (9), and in particular that $G^K = -G^R[G^{-1}]^K G^A$, one may write:

$$G^K(\nu) = -\frac{2i\gamma}{[(\nu + i\gamma)^2 - E_i^2][(\nu - i\gamma)^2 - E_i^2]} \times \begin{pmatrix} \nu - \tilde{\epsilon}_i + i\gamma & -g_i\psi_0 \\ -g_i\psi_0 & \nu + \tilde{\epsilon}_i + i\gamma \end{pmatrix} \begin{pmatrix} F_B(\nu) & 0 \\ 0 & F_A(\nu) \end{pmatrix} \begin{pmatrix} \nu - \tilde{\epsilon}_i - i\gamma & -g_i\psi_0 \\ -g_i\psi_0 & \nu + \tilde{\epsilon}_i - i\gamma \end{pmatrix}. \quad (31)$$

For the mean-field condition in Eq. (12), we require in particular the $G_{a_i^\dagger b_i}^K$ component which has the form:

$$G_{a_i^\dagger b_i}^K(\nu) = 2i\gamma g\psi_0 \frac{[F_A(\nu) + F_B(\nu)]\nu + [F_B(\nu) - F_A(\nu)](\tilde{\epsilon}_i + i\gamma)}{[(\nu - E_i)^2 + \gamma^2][(\nu + E_i)^2 + \gamma^2]}. \quad (32)$$

4 Mean-field theory and its limits

Putting the $G_{a_i^\dagger b_i}^K$ component of Eq. (32) into Eq. (20) gives the self-consistency condition (equation for the condensate) of the mean-field theory:

$$(\omega_0 - \mu_S - i\kappa)\psi_0 = \sum_i g_i^2 \psi_0 \gamma \int \frac{d\nu}{2\pi} \frac{(F_B + F_A)\nu + (F_B - F_A)(\tilde{\epsilon}_i + i\gamma)}{[(\nu - E_i)^2 + \gamma^2][(\nu + E_i)^2 + \gamma^2]}. \quad (33)$$

Equation (33) is central to our analysis. This equation is rather powerful, in that it combines several well known theoretical results within a single framework. As will be shown in section 4, in the equilibrium limit (where the system–bath couplings are taken to zero) Eq. (33) reduces to the gap equation which applies throughout the BCS–BEC crossover. In the opposite highly non-equilibrium limit (see section 4) it reduces to the standard laser condition. At low densities it reduces to the (complex) Gross-Pitaevskii equation, discussed in section 4. As such, this approach highlights the connections between these apparently different descriptions of condensates or lasers.

The functions $F_{A,B}$ appearing in Eq. (33) were defined as $F_{A,B} = 1 - 2n_{A,B}$, where $n_{A,B}$ are bath occupation functions. These occupations are taken to be externally imposed, and can be chosen to have any form relevant to a particular physical situation. Here, we will choose these to be thermal and at equal temperatures but different chemical potentials. Noting that the fermionic states were supposed to represent two-level systems (or excitons), we take the occupations to satisfy $n_A + n_B = 1$. This therefore requires that we have:

$$F_{A,B}(\nu) = \tanh \left[\frac{\beta}{2} \left(\nu \pm \frac{\mu_B - \mu_S}{2} \right) \right], \quad (34)$$

where μ_B is an adjustable pumping bath chemical potential, and μ_S appears in this expression due to the shift arising from the gauge transformation in Eq. (22). Schematically, this situation is illustrated in Fig. 0.3; one can see that $F_A(-\epsilon) + F_B(\epsilon) = 2[1 - n_A(-\epsilon) - n_B(\epsilon)] = 0$. Physically, this pumping process is most closely related to electrical pumping. Note that, in the absence of any other processes, contact between the two-level systems (excitons) and the pumping reservoir would control the population of the two-level systems, and so one would have:

$$\langle b^\dagger b - a^\dagger a \rangle = n_B(\epsilon) - n_A(-\epsilon) = -\tanh \left[\frac{\beta}{2} \left(\epsilon - \frac{\mu_B}{2} + \frac{\mu_S}{2} \right) \right].$$

Thus, by pumping with a thermalised bath, one will find a thermalised distribution of excitons. Therefore, in the context of polaritons this pumping scheme resembles closely pumping from a thermalised excitonic reservoir, which is often the case in the experiments.

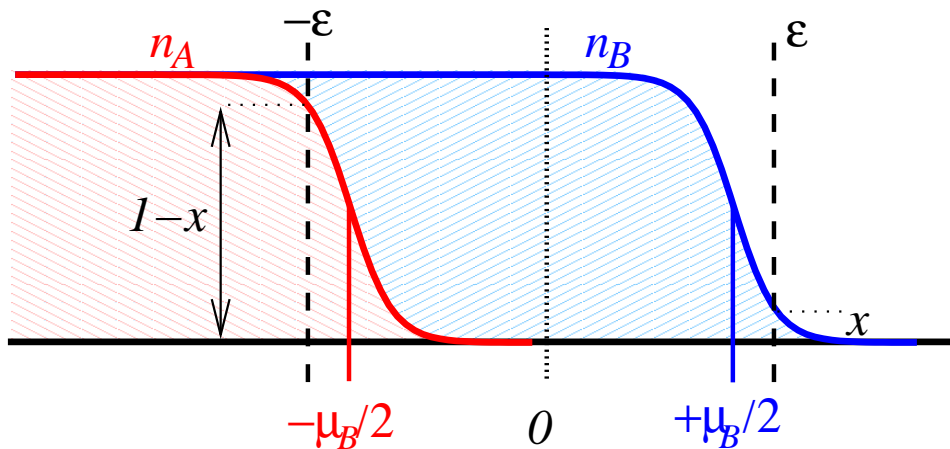


Figure 0.3: Occupation functions for the pumping baths, chosen to set total occupation of two modes to one, while varying the degree of inversion.

Equilibrium limit of Mean-field theory

The simplest limit to recover from the non-equilibrium self-consistency equation is that of thermal equilibrium. This corresponds to taking $\gamma, \kappa \rightarrow 0$. Since the self-consistency equation included only the coupling between mean-field photons and the decay bath, there is no way that a thermal distribution can be set by the decay bath. On the other hand, the pumping bath can set a thermal distribution, so to recover a non-trivial equilibrium distribution one should take $\kappa \rightarrow 0$ first, and then $\gamma \rightarrow 0$. If $\kappa = 0$, then the imaginary part of the right hand side of Eq. (33) must vanish. In order to satisfy this, without restricting the range of solutions of the real part, one must choose $F_B(\nu) = F_A(\nu)$. In terms of the distribution functions written in Eq. (34), this clearly means $\mu_S = \mu_B$. Physically, this means that in the absence of decay, the chemical potential of the condensate matches the pumping bath.

After fixing μ_S , the remaining part of the equation becomes:

$$(\omega_0 - \mu_B)\psi_0 = \sum_i g_i^2 \psi_0 \gamma \int \frac{d\nu}{2\pi} \frac{2 \tanh(\beta\nu/2) \nu}{[(\nu - E_i)^2 + \gamma^2][(\nu + E_i)^2 + \gamma^2]}. \quad (35)$$

We may then take the limit of small γ , by using:

$$\lim_{\gamma \rightarrow 0} \frac{2\gamma\nu}{[(\nu - E_i)^2 + \gamma^2][(\nu + E_i)^2 + \gamma^2]} = \frac{2\pi}{4E_i} [\delta(\nu - E_i) - \delta(\nu + E_i)], \quad (36)$$

hence we find:

$$\begin{aligned} (\omega_0 - \mu_B)\psi_0 &= \sum_i \frac{g_i^2 \psi_0}{4E_i} \int d\nu \tanh\left(\frac{\beta\nu}{2}\right) [\delta(\nu - E_i) - \delta(\nu + E_i)] \\ &= \sum_i \frac{g_i^2 \psi_0}{2E_i} \tanh\left(\frac{\beta E_i}{2}\right). \end{aligned} \quad (37)$$

This is the equilibrium result[51–53], but with the two-level constraint on the fermions imposed only on average.¹ Note, that this is the standard mean-field gap equation of the BCS-BEC crossover theory [56].

High temperature limit of Mean-field theory - simple laser

The opposite extreme to the equilibrium condensate is the limit of a simple laser, which can also be recovered from Eq. (33). Before showing how this limit can be recovered from our theory, we first provide a brief summary of the threshold condition of a simple laser, and express it in similar language to the above self-consistency condition. The equations describing the steady state of a laser can be derived starting from the well-known Maxwell-Bloch equations:

$$\partial_t \psi_0 = -i\omega_0 \psi_0 - \kappa \psi_0 + \sum_i g_i P_i, \quad (39)$$

$$\partial_t P_i = -2i\epsilon_i P_i - \lambda_\perp P_i + g_i \psi_0 N_i \quad (40)$$

$$\partial_t N_i = \lambda_\parallel (N_0 - N_i) - 2g_i (\psi_0^* P_i + P_i^* \psi_0). \quad (41)$$

These equations can be understood as originating from considering a Hamiltonian like Eq. (1), with $P_i = -i\langle a_i^\dagger b_i \rangle$, $N_i = \langle b_i^\dagger b_i - a_i^\dagger a_i \rangle$. One then writes the Heisenberg-Langevin equations, with a Markovian set of baths distinct for each two-level system, and then takes the semiclassical approximation to drop bath noise operators. The value N_0 is the bath inversion imposed by the pumping. Note that with coupling to such a Markovian pumping bath, there is a discontinuous jump between the allowed steady states with no decay, and the laser-like solutions found for any non-zero pumping[57]. In particular, with pumping and decay, inversion is always required for a condensed solution of these Maxwell-Bloch equations, so they cannot smoothly interpolate between a condensate and a laser. Such behaviour should not be too surprising, as a frequency independent (Markovian) bath occupation corresponds to an infinite temperature, and so even arbitrarily weak coupling of the system to an infinite temperature reservoir may destroy the condensate. With more realistic models of pumping, such a discontinuous jump need not necessarily occur. One should thus interpret the microscopic origin and consequent behaviour of Eqs. (39– 41) with some caution. However, since Maxwell-Bloch equations of the above form are frequently used as a simple model of a laser, it is instructive to see what approximations they would correspond to in terms of our non-equilibrium formalism, in which the microscopic description of the pumping is better controlled.

Starting from these Maxwell-Bloch equations, the self-consistency condition for a macroscopic photon field $\psi_0(t) = \psi_0 e^{-i\mu t}$ can be written as:

$$(-i\mu + i\omega_0 + \kappa)\psi_0 = \sum_i g_i P_i, \quad (-i\mu + 2i\epsilon_i + \lambda_\perp)P_i = g_i \psi_0 N_i, \quad (42)$$

which can be combined to write a single self-consistency condition:

$$(\omega_0 - \mu - i\kappa)\psi_0 = - \sum_i \frac{g_i^2 \psi_0 N_i}{2\tilde{\epsilon}_i - i\lambda_\perp}. \quad (43)$$

¹Imposing the two-level constraint on average, the equilibrium expectation of the inversion $\langle b^\dagger b - a^\dagger a \rangle$ can be written as:

$$\frac{e^{\beta E} - e^{-\beta E}}{1 + e^{\beta E} + e^{-\beta E} + 1} = \frac{(e^{\beta E/2} - e^{-\beta E/2})(e^{\beta E/2} + e^{-\beta E/2})}{(e^{\beta E/2} + e^{-\beta E/2})^2} = \tanh\left(\frac{\beta E}{2}\right). \quad (38)$$

Were the two-level constraint imposed exactly, the result would instead be: $(e^{\beta E} - e^{-\beta E})/(e^{\beta E} + e^{-\beta E}) = \tanh(\beta E)$, as the zero and doubly occupied states would be removed from the denominator.

Substituting the steady state value of P_i from Eq. (42) into Eq. (41) gives:

$$N_0 = N_i \left[1 + \frac{2g_i^2 |\psi_0|^2}{\lambda_{\parallel}} \frac{2\lambda_{\perp}}{\lambda_{\perp}^2 + 4\tilde{\epsilon}_i^2} \right] \quad (44)$$

hence we may substitute this into Eq. (43) to give the final form of the self-consistency condition for the Maxwell-Bloch equations:

$$(\omega_0 - \mu - i\kappa)\psi_0 = - \sum_i g_i^2 \psi_0 N_0 \frac{(2\tilde{\epsilon}_i + i\lambda_{\perp})}{[4\tilde{\epsilon}_i^2 + \lambda_{\perp}^2 + 4(\lambda_{\perp}/\lambda_{\parallel})g_i^2 |\psi_0|^2]}. \quad (45)$$

The laser threshold condition is given by taking $\psi \rightarrow 0$ in the above equation. If we also take $g_i = g$, $\epsilon_i = \epsilon$, and the usual laser operating condition of $\lambda_{\perp} \gg \kappa$ one has that lasing occurs at the cavity frequency, $\mu = \omega_0$ and the threshold condition has the well-known form: $\kappa\lambda_{\perp}/g^2 = nN_0$, where n is the number of two-level systems.

Recovering laser limit from non-equilibrium mean-field theory

This simple laser self-consistency condition can be recovered from equation (33) if rather than using the frequency dependent forms for $F_{A,B}(\nu)$ discussed previously, one instead takes $F_{A,B}$ to be constants. Physically such a limit corresponds to high temperatures. Note that as the temperature rises, to keep the bath population fixed, the chemical potential must also vary. We will therefore take $\mu \propto T$, and then take the limit $T \rightarrow \infty$. Such a limit has another simple interpretation, corresponding to making a fully Markovian approximation, including assuming the occupation, as well as the density of states, to be flat, and so writing the Keldysh part of the self energy as

$$\Sigma_{a^{\dagger}a}^{--}(t, t') = -i \sum_n \Gamma_{i,n}^2 [1 - 2n_F(\nu_n^{\Gamma})] e^{-i\nu_n^{\Gamma}(t-t')} = -2i\gamma F_A \delta(t - t'). \quad (46)$$

As such, our approach in Eq. (29) is Markovian for the density of states of the bath, but non-Markovian for the occupation. In terms of quantum statistical (i.e. Heisenberg-Langevin) approaches, the distinction is whether the noise should be taken as white noise or coloured noise. Assuming the noise correlations to be white, and thus neglecting the frequency dependence of occupation, is also the approximation underlying the quantum regression theorem[49], which allows one to relate two-time correlations to the evolution of the density matrix. The role of this approximation, and its implications for the fluctuation dissipation theorem are discussed by Ford and O'Connell[50].

If $F_{A,B}$ are frequency independent, then in Eq. (33), the term in the integral proportional to ν will vanish as this is an odd function, and so Eq. (33) becomes:

$$(\omega_0 - \mu - i\kappa)\psi_0 = \sum_i g_i^2 \psi_0 (F_B - F_A) \frac{\tilde{\epsilon}_i + i\gamma}{4(E_i^2 + \gamma^2)}. \quad (47)$$

Hence, the polarisation of the two-level systems is in this case proportional to the inversion of the baths, $N_0 = (n_B - n_A) = -(F_B - F_A)/2$ and we have:

$$(\omega_0 - \mu - i\kappa)\psi_0 = - \sum_i g_i^2 \psi_0 N_0 \frac{\tilde{\epsilon}_i + i\gamma}{2(E_i^2 + \gamma^2)}. \quad (48)$$

Then, identifying the decay constants in Eq. (45) as $\lambda_{\perp} = \lambda_{\parallel} = 2\gamma$, Eq. (48) and Eq. (45) are equivalent.

General properties of mean-field theory away from extremes

Away from the extremes of laser theory or of thermal equilibrium, the effect of pumping on the phase boundary can be understood as a result of competition of two effects: pumping and decay add noise, reducing coherence, hence suppressing condensation; on the other hand, for a given decay rate, pumping increases the density, favouring condensation. The simplest illustration of the first of these is shown in Fig. 0.4, where one sees that as the value of γ is increased, for a fixed κ , the critical density required for condensation increases.

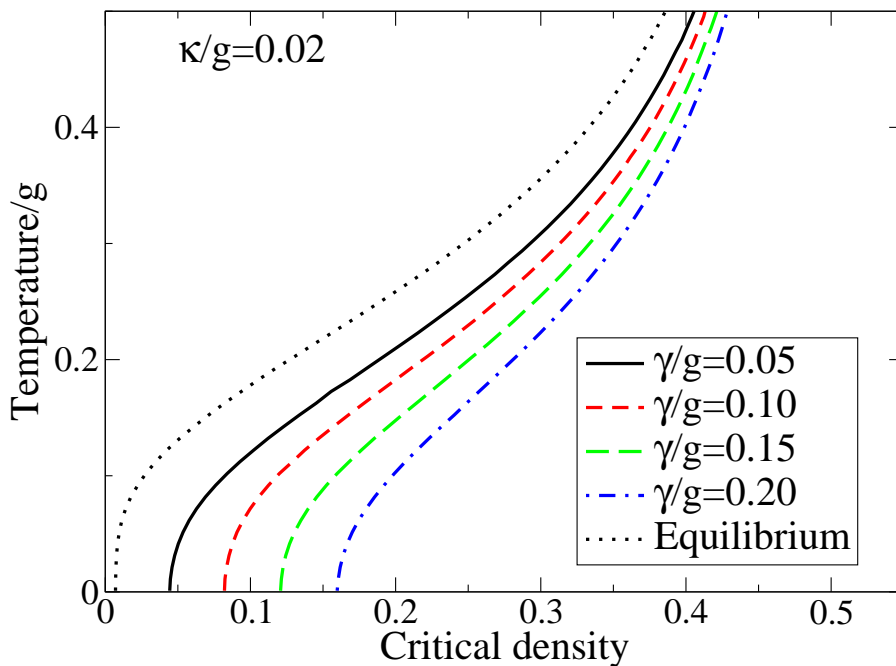


Figure 0.4: Critical temperature as a function of density, showing effects of pumping and decay, taking a Gaussian distribution of two-level-system energies with variance $0.15g$. Adapted from Ref.[29].

To see the competition between pumping causing dephasing and pumping increasing density, one may look at the low temperature limit, shown in Fig. 0.5, plotting the critical value of κ as a function of γ . Two lines are shown; the solid line has an inverted bath (as would be required for the laser limit), the dashed line has a non-inverted bath. In the later case (as illustrated in the inset) for small γ , the two-level system energy is too far below the pumping bath, and insufficiently broadened by γ , to be populated; for larger γ the broadening is sufficient, and condensation may occur. In the presence of inhomogeneous broadening, the above picture is significantly relaxed, since the tail of the density of states can be occupied even if the peak is below the chemical potential.

Low density limit: recovering complex Gross-Pitaevskii equation

The self-consistency condition of Eq. (33) can also be related to the idea of the complex Gross-Pitaevskii equation providing a mean-field description of a spatially varying condensate. For a steady uniform state, the mean-field self-consistency condition may be understood as $(\mu_S + i\kappa - \omega_0)\psi_0 = \chi[\psi_0, \mu_S]\psi_0$, where $\chi[\psi_0, \mu_S]$ is a nonlinear complex susceptibility. For a $\psi_0(r, t)$ which varies slowly in space and time [up to an allowed fast time dependence described by a

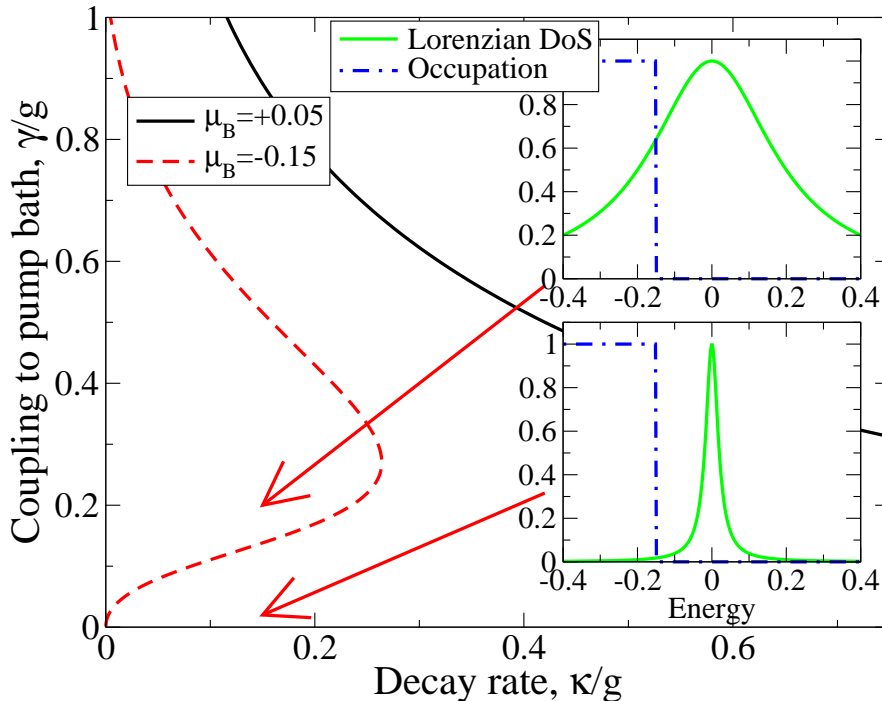


Figure 0.5: Critical couplings to pumping bath without inhomogeneous broadening and at low temperatures.

factor $\exp(-i\mu_B t)$, one may consider the local density approximation:

$$\left(i\partial_t + i\kappa - \left[V(r) - \frac{\nabla^2}{2m} \right] \right) \psi_0(r, t) = \chi[\psi_0(r, t)]\psi_0(r, t). \quad (49)$$

In order to determine the large scale spatial structure of a condensate, or its low energy collective modes, it is often sufficient to make a Taylor expansion of the nonlinear complex susceptibility, resulting in a complex Gross-Pitaevskii equation:

$$i\partial_t \psi_0 = \left(-\frac{\nabla^2}{2m} + V(r) + U|\psi_0|^2 + i[\gamma_{\text{eff}}(\mu_B) - \kappa - \Gamma|\psi_0|^2] \right) \psi_0, \quad (50)$$

where Γ represents the simplest form of nonlinearity of the imaginary part, taking a form that will ensure stability.

Depending on the details of pumping included in the model, one may find that by treating $\chi[\psi(t)]$ more carefully the susceptibility depends not only on the current value of $\psi(t)$, but on its history, due to dynamics of the reservoir. [In fact, to correctly reproduce the polariton spectrum, one ought to take the excitonic susceptibility to have a resonance at the exciton energy, after which a variant of Eq. (50), but with the appropriate polariton dispersion will be recovered.] In the limit of sufficiently slow dynamics of the system, or when considering steady states, dynamics of the reservoir should become unimportant. Results of the complex Gross-Pitaevskii equation with or without separate reservoir dynamics may be found elsewhere[45–47]

5 Fluctuations, and instability of the normal state

As stated earlier, when introducing the self-consistency condition for the non-equilibrium problem, it is not possible to consider minimising free energy when looking at a system coupled to

multiple baths, and so it is instead necessary to look for stable steady states. The self consistency conditions discussed above determine whether a steady state may exist, but not whether it is stable. In order to analyse stability, it is necessary to consider fluctuations about a given state, and to find whether they grow or decay in time. In addition, the study of fluctuations allows one to determine the response functions of the system — in the present context, this means the photon Green's function — which in turn will give the physical observables, such as photoluminescence and absorption spectra.

In the non-equilibrium case, both the spectrum of possible excitations (i.e. what is seen in the absorption spectrum), and its occupation (i.e. photoluminescence) must be determined independently, for which the Keldysh Green's function approach is ideal. In the following, the approach to calculating these Green's functions is discussed for both the normal and condensed state, and then this approach is applied to understanding the instability of the normal state, which allows a clearer interpretation of the relation between the non-equilibrium condensate and a simple laser. For the condensed system, the calculations are more complicated due to the existence of non-zero anomalous correlations, i.e. $\langle \psi_k(t)\psi_{-k}(t') \rangle$; the general structure of the spectrum of the non-equilibrium system will be discussed in section 6.

Photon Green's functions in the non-equilibrium model

To allow for anomalous correlations in the condensed state, it is helpful to write the Green's function in a vector space of $\psi_k, \psi_{-k}^\dagger$. Just as in the above discussion of the Green's functions for the two-level system, this vector space of $\psi_k, \psi_{-k}^\dagger$ should be combined with the \pm space due to the Keldysh/retarded/advanced structure. Thus, one has four by four matrices, in the basis $(\psi_{k,+}, \psi_{-k,+}^\dagger, \psi_{k,-}, \psi_{-k,-}^\dagger)$.

The photon Green's function can be found by solving the Dyson equation, $D^{-1} = D_0^{-1} - \Sigma$, and so to start with, the free photon Green's function is required. The free Hamiltonian in this case is just $H_0^{\text{photon}} = \sum_k \omega_k \psi_k^\dagger \psi_k$. In the four by four basis arising from mixing $\psi_k, \psi_{-k}^\dagger$, some elements correspond to Green's functions in which ψ, ψ^\dagger are interchanged in order. This means that these elements are Hermitian conjugated, giving the form:

$$D_0^{-1} = \begin{pmatrix} 0 & 0 & \omega - \tilde{\omega}_k - i\eta & 0 \\ 0 & 0 & 0 & -\omega - \tilde{\omega}_k + i\eta \\ \omega - \tilde{\omega}_k + i\eta & 0 & (2i\eta)F_0(\omega + \mu) & 0 \\ 0 & -\omega - \tilde{\omega}_k - i\eta & 0 & (2i\eta)F_0(-\omega + \mu) \end{pmatrix}, \quad (51)$$

where once again η is infinitesimal. In this, we have written all frequencies measured relative to μ_S , meaning that we made the substitution $\psi_k \rightarrow e^{-i\mu_S t}(\psi_0 \delta_{k,0} + \psi_k)$.

To this free Green's function one must add self energies arising from two parts of the interaction Hamiltonian. The first is the coupling between cavity photons and the decay bath; the second is the coupling between the photons and the pumped two-level systems. The first contribution has a form exactly analogous to the coupling between the two-level systems and pumping baths, i.e.:

$$\begin{aligned} \Sigma_{\psi^\dagger\psi}^{++}(t, t') &= \sum_p \zeta_{p,k}^2 D_{\Psi^\dagger\Psi}^{--} = 0 \\ \Sigma_{\psi^\dagger\psi}^{-+}(t, t') &= \sum_p \zeta_{p,k}^2 D_{\Psi^\dagger\Psi}^{+-} = -i \sum_p \zeta_{p,k}^2 \theta(t - t') e^{-i\omega_p^\zeta(t-t')} = -i\kappa\delta(t - t') \\ \Sigma_{\psi^\dagger\psi}^{+-}(t, t') &= \sum_p \zeta_{p,k}^2 D_{\Psi^\dagger\Psi}^{-+} = +i \sum_p \zeta_{p,k}^2 \theta(t' - t) e^{+i\omega_p^\zeta(t-t')} = +i\kappa\delta(t - t') \\ \Sigma_{\psi^\dagger\psi}^{--}(t, t') &= \sum_p \zeta_{p,k}^2 D_{\Psi^\dagger\Psi}^{++} = -i \sum_p \zeta_{p,k}^2 [2n_\Psi(\omega_p^\zeta) + 1] e^{-i\omega_p^\zeta(t-t')} = -2i\kappa\check{F}_\Psi(t - t'), \end{aligned}$$

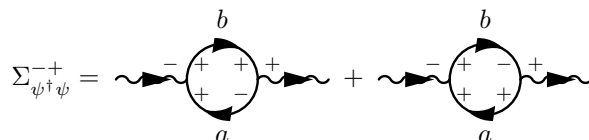
where as before \check{F}_Ψ is the Fourier transform of the $2n_\Psi(\omega) + 1$, and the Markovian limit for the bath density of states and coupling constant has been applied to get the final expression; these terms thus give a self energy:

$$\Sigma_{\text{decay}}(\omega) = \begin{pmatrix} 0 & 0 & +i\kappa & 0 \\ 0 & 0 & 0 & -i\kappa \\ -i\kappa & 0 & -(2i\kappa)F_\Psi(\omega + \mu_S) & 0 \\ 0 & +i\kappa & 0 & -(2i\kappa)F_\Psi(-\omega + \mu_S) \end{pmatrix}. \quad (52)$$

In calculating the self energy due to the coupling to two-level systems, one may simplify the calculation by noting that only $\Sigma_{\psi^\dagger\psi}^R, \Sigma_{\psi^\dagger\psi^\dagger}^R, \Sigma_{\psi^\dagger\psi}^K, \Sigma_{\psi^\dagger\psi^\dagger}^K$ are independent; all other self energies can be related to these quantities by Hermitian conjugation and/or swapping $\omega \rightarrow -\omega$. To generate the diagrams for these self energies, we should first determine the interaction vertices that give rise to such self energies. The relevant part of the interaction Hamiltonian here is the interaction between two-level systems and incoherent photons, and so the relevant contribution to U comes from

$$\begin{aligned} \int_C dt \tilde{H}_{\text{int}}^{\text{TLS-photon}} &= \int_{-\infty}^{\infty} dtg \left[\tilde{\psi}(t, f) \tilde{b}_i^\dagger(t, f) \tilde{a}_i(t, f) - \tilde{\psi}(t, b) \tilde{b}_i^\dagger(t, b) \tilde{a}_i(t, b) + \text{H.c.} \right] \\ &= \int_{-\infty}^{\infty} dt \frac{g}{\sqrt{2}} \left[\tilde{\psi}_+(t) \left(\tilde{b}_{i+}^\dagger(t) \tilde{a}_{i-}(t) + \tilde{b}_{i-}^\dagger(t) \tilde{a}_{i+}(t) \right) \right. \\ &\quad \left. + \tilde{\psi}_-(t) \left(\tilde{b}_{i+}^\dagger(t) \tilde{a}_{i+}(t) + \tilde{b}_{i-}^\dagger(t) \tilde{a}_{i-}(t) \right) + \text{H.c.} \right]. \end{aligned} \quad (53)$$

The self energy diagrams thus consist of diagrams with one incoming and one outgoing photon line, connected via the interaction vertices in Eq. (53), and the Green's functions for the two-level system. As is clear from Eq. (53), the vertices all involve the two-level system swapping between the a and b states. Just as for the diagrams describing the effects of the bath discussed in Sec. 3, one must also keep track of the \pm labels on the fields. To calculate, for instance, the retarded self energy (i.e. the $-+$ component) it is clear that the vertices arising from the possible placements of \pm signs have the form:



(any other set of possible \pm labels on the internal lines will involve a $--$ line, and such Green's functions vanish). To translate these diagrams into an equation for the self energy, one must use the following Feynman rules (see Refs.[31–33]): For each interaction vertex there is a factor $(-ig/\sqrt{2})$, and for each internal Green's function, a factor iG . There is then a prefactor $i(-1)^F$, where F is the number of closed Fermion loops ($F = 1$ in the current case), and there is a combinatoric factor associated with how the vertices are found from the expansion of U , which is the same as in any other diagrammatic approach. Applying these rules, one may write:

$$\Sigma_{\psi^\dagger\psi}^{-+} = -i \frac{2}{2!} \left(\frac{g}{\sqrt{2}} \right)^2 \int \frac{d\nu}{2\pi} \sum_i \left[G_{a_i^\dagger a_i}^A(\nu) G_{b_i^\dagger b_i}^K(\nu + \omega) + G_{a_i^\dagger a_i}^K(\nu) G_{b_i^\dagger b_i}^R(\nu + \omega) \right]. \quad (54)$$

For the anomalous case, all that changes is the a, b labels, i.e.:

$$\Sigma_{\psi^\dagger\psi^\dagger}^{-+} = -i \frac{2}{2!} \left(\frac{g}{\sqrt{2}} \right)^2 \int \frac{d\nu}{2\pi} \sum_i \left[G_{a_i^\dagger b_i}^A(\nu) G_{b_i^\dagger a_i}^K(\nu + \omega) + G_{a_i^\dagger b_i}^K(\nu) G_{b_i^\dagger a_i}^R(\nu + \omega) \right]. \quad (55)$$

The component Σ^{+-} is just the Hermitian conjugate of Σ^{-+} as above. The component Σ^{++} vanishes, since it either involves $--$ lines, or it involves products of two retarded Green's

functions. Since the retarded Green's function is causal — i.e. $D^R(t, t') \propto \theta(t - t')$ — then as a function of frequency, all of its poles are in the lower half plane, and so the integral of a product of two such functions is equal to zero.² The only other surviving component of the self energy is thus:

which gives the equation:

$$\begin{aligned} \Sigma_{\psi^\dagger\psi}^{--} = & -i \frac{2}{2!} \left(\frac{g}{\sqrt{2}} \right)^2 \int \frac{d\nu}{2\pi} \sum_i \left[G_{a_i^\dagger a_i}^K(\nu) G_{b_i^\dagger b_i}^K(\nu + \omega) + G_{a_i^\dagger a_i}^A(\nu) G_{b_i^\dagger b_i}^R(\nu + \omega) \right. \\ & \left. + G_{a_i^\dagger a_i}^R(\nu) G_{b_i^\dagger b_i}^A(\nu + \omega) \right]. \end{aligned} \quad (56)$$

As was the case for the retarded components, the only difference between normal and anomalous Keldysh components is in the a, b labels, so:

$$\begin{aligned} \Sigma_{\psi^\dagger\psi^\dagger}^{--} = & -i \frac{2}{2!} \left(\frac{g}{\sqrt{2}} \right)^2 \int \frac{d\nu}{2\pi} \sum_i \left[G_{a_i^\dagger b_i}^K(\nu) G_{b_i^\dagger a_i}^K(\nu + \omega) + G_{a_i^\dagger b_i}^A(\nu) G_{b_i^\dagger a_i}^R(\nu + \omega) \right. \\ & \left. + G_{a_i^\dagger b_i}^R(\nu) G_{b_i^\dagger a_i}^A(\nu + \omega) \right]. \end{aligned} \quad (57)$$

Combining the self energies due to the pumped two-level systems and the self energy due to decay with the free inverse Green's function, one can then find expressions for the photon Green's functions, and hence observable quantities such as the photoluminescence intensity as a function of frequency and momentum, which is given by $\mathcal{L}(\omega) = i \left(D_{\psi^\dagger\psi}^K - D_{\psi^\dagger\psi}^R + D_{\psi^\dagger\psi}^A \right) / 2$. In section 5, the normal state Green's functions are studied: we show how an effective density of states and occupation function can be defined, and also show how the behaviour of these functions can be related to the structure of the inverse Green's function, and to the stability of the normal system.

In the condensed state, just as in equilibrium, the form of the inverse Green's function can be shown to obey the Hugenholtz-Pines relation[58] (see also [59, Chapter 6]), meaning that $[D_{\psi^\dagger\psi}^R]^{-1}(0, 0) = [D_{\psi^\dagger\psi^\dagger}^R]^{-1}(0, 0)$, which implies there is a gapless spectrum. Just as in equilibrium, one may show that the requirement for the Hugenholtz-Pines relation to be satisfied is equivalent to the mean-field condition, Eq. (33). It is worth noting that as $\psi_0 \rightarrow 0$, the Hugenholtz-Pines relation (and hence the mean-field condition) become equivalent to the condition that:

$$[D_{\psi^\dagger\psi}^R]^{-1}(\omega = \mu_{\text{eff}}, k = 0) = \mu_{\text{eff}} - \omega_0 + i\kappa - \Sigma_{\text{TLS}}^R(\mu_{\text{eff}}) = 0, \quad (58)$$

for some particular μ_{eff} . (In this expression, the non-condensed self energies have been written without the gauge transform of Eq. (22), as in the absence of a condensate, there is no reason to perform the gauge transformation.) Section 5 will show that the condition in Eq. (58) also corresponds to the point when the normal state ceases to be stable.

²NB; since the Green's function generically looks like $1/\omega$ at large ω , the integral of a single retarded Green's function depends on the regularisation used. However, for a product of retarded Green's functions, the integral is well defined, and so vanishes.

Normal-state Green's functions and instability

Focusing on the non-condensed case, the properties of the spectrum are entirely determined by three real functions of ω , as one may write:

$$\left[D_{\psi^\dagger\psi}^R \right]^{-1}(\omega) = A(\omega) + iB(\omega), \quad \left[D_{\psi^\dagger\psi}^{-1} \right]^K(\omega) = iC(\omega). \quad (59)$$

The forms of $A(\omega), B(\omega), C(\omega)$ follow from the expressions in the previous section. These somewhat simplify since we are considering the normal case, and so one has:

$$\left[D_{\psi^\dagger\psi}^R \right]^{-1}(\omega) = \omega - \omega_k + i\kappa - \Sigma_{\text{TLS}}^R(\omega), \quad \left[D_{\psi^\dagger\psi}^{-1} \right]^K(\omega) = 2i\kappa F_\Psi(\omega) - \Sigma_{\text{TLS}}^K(\omega), \quad (60)$$

where $\Sigma_{\text{TLS}}^{R,K}$ are the self energies from the pumped two-level systems given by Eq. (54) and Eq. (56). In the following we will first discuss how the forms of $A(\omega), B(\omega), C(\omega)$ determine the spectrum, occupation and stability, and then illustrate this with their forms arising from the particular microscopic model discussed above.

Inverting the matrix of Keldysh Green's functions (using Eq. (9)), one finds:

$$D_{\psi^\dagger\psi}^R(\omega) = \frac{A(\omega) - iB(\omega)}{A(\omega)^2 + B(\omega)^2}, \quad D_{\psi^\dagger\psi}^K(\omega) = \frac{-iC(\omega)}{A(\omega)^2 + B(\omega)^2}, \quad (61)$$

and then in terms of these quantities, we may write the luminescence spectrum:

$$\mathcal{L}(\omega) = \frac{i}{2} \left[D_{\psi^\dagger\psi}^K(\omega) - \left(D_{\psi^\dagger\psi}^R(\omega) - D_{\psi^\dagger\psi}^A(\omega) \right) \right] = \frac{C(\omega) - 2B(\omega)}{2[A(\omega)^2 + B(\omega)^2]}. \quad (62)$$

Further, by analogy with the equilibrium system, we can explain the form of this expression in terms of a spectral weight (density of states) $\rho(\omega) = -2\Im[D_{\psi^\dagger\psi}^R(\omega)]$ and an occupation function $2n_\psi(\omega) + 1 = iD_{\psi^\dagger\psi}^K(\omega)/\rho(\omega)$, giving:

$$\rho(\omega) = \frac{2B(\omega)}{A(\omega)^2 + B(\omega)^2}, \quad n_\psi(\omega) = \frac{1}{2} \left[\frac{C(\omega)}{2B(\omega)} - 1 \right], \quad (63)$$

hence the luminescence is related to these as $\mathcal{L}(\omega) = \rho(\omega)n_\psi(\omega)$ as expected.

In the absence of coupling to the two-level systems (and hence neglecting $\Sigma_{\text{TLS}}^{R,K}$ in Eq. (60), one may clearly identify the role of the three expressions involved here:

- $B(\omega) = \kappa$ is the linewidth of the normal modes
- $A(\omega) = \omega - \omega_k$ describes the locations of these modes, and
- $C(\omega) = 2\kappa(2n_\psi + 1)$ describes their occupation.

However, when coupled to the two-level systems, $B(\omega)$ is not a constant, hence firstly, the linewidth varies, and more importantly, $B(\omega)$ may vanish at some value of ω . If $B(\omega)$ does vanish then the occupation diverges, but since the spectral weight vanishes too, the luminescence remains finite.

Physically, this describes the behaviour that would, in equilibrium, be expected at the chemical potential, as long as the chemical potential lies below the bottom of the band. Note that the equilibrium Bose-Einstein distribution diverges at the chemical potential. However, if the chemical potential lies below the bottom of the band then the spectral weight is zero at the chemical potential and thus the particle number (luminescence) remains finite.

Out of equilibrium, the system distribution may in general be far from the Bose-Einstein distribution. Even so, when near the threshold for condensation, the system distribution shares

an important property with the Bose-Einstein distribution: near the frequency where the condensate will emerge [i.e near the point where $B(\omega) = 0$] the system distribution will diverge as $1/(\omega - \mu_{\text{eff}})$, just as the Bose-Einstein distribution does. We may thus identify the effect of pumping as introducing a chemical potential that has nothing to do with the chemical potential of the decay bath. Since $B(\omega)$ is given by the inverse retarded Green's function, one may note that the inverse Keldysh Green's function does not on its own fix the distribution; it is the ratio of Keldysh and imaginary retarded Green's functions that matter. Figure 0.6 shows how the spectral weight, occupation and luminescence are related to the zeros of the real and imaginary parts of the inverse Green's function.

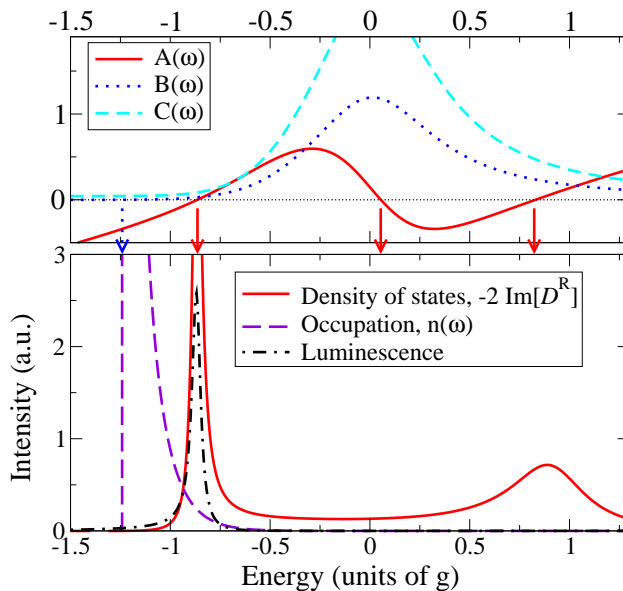


Figure 0.6: Behaviour of inverse Green's functions, and resulting properties of spectral weight, luminescence and occupation functions in the normal state. Upper panel shows the inverse Green's functions (with zeros marked by arrows), and the lower panel shows the various physical correlations of interest. Adapted from Ref.[29].

Zeros of $A(\omega)$, $B(\omega)$ and stability

Although a zero of $B(\omega)$ alone does not cause the luminescence to diverge, a simultaneous zero of $A(\omega)$ and $B(\omega)$ will. The stability of the system can be seen to change when this occurs, as will be discussed next. When near a simultaneous zero, one may expand $A(\omega) = \alpha(\omega - \xi)$, and $B(\omega) = \beta(\omega - \mu_{\text{eff}})$, and so:

$$\begin{aligned} [D_{\psi^\dagger\psi}^R]^{-1}(\omega) &\simeq \alpha(\omega - \xi) + i\beta(\omega - \mu_{\text{eff}}) \\ &= (\alpha + i\beta) \left[\omega - \frac{(\alpha\xi + i\beta\mu_{\text{eff}})(\alpha - i\beta)}{\alpha^2 + \beta^2} \right], \end{aligned} \quad (64)$$

hence the actual poles are at frequencies:

$$\omega^* = \frac{(\alpha^2\xi + \beta^2\mu_{\text{eff}}) + i\alpha\beta(\mu_{\text{eff}} - \xi)}{\alpha^2 + \beta^2}. \quad (65)$$

These poles determine the time dependence of the retarded Green's function, so if $\mu_{\text{eff}} > \xi$, then the pole has the wrong sign of imaginary part and the normal state is unstable. When $\mu_{\text{eff}} = \xi$, then this means there is a value $\omega = \mu_{\text{eff}} = \xi$ for which $[D_{\psi^\dagger\psi}^R]^{-1}(\omega, k = 0) = 0$, which as

discussed in Eq. (58) is equivalent to saying that the mean-field consistency condition can be satisfied. Hence, instability of the normal state, and the existence of a condensed solution will occur together.

It is helpful here to explicitly write $B(\omega)$, in order to understand the origin of its zeros, and what parameters determine their location. In the non-condensed case, the fermionic Green's functions that come from inverting Eq. (30) have a simple form:

$$G_{b^\dagger b, a^\dagger a}^R = \frac{1}{\nu \mp \epsilon_i + i\gamma}, \quad G_{b^\dagger b, a^\dagger a}^K = -\frac{2i\gamma F_{B,A}(\nu)}{(\nu \mp \epsilon_i)^2 + \gamma^2}, \quad (66)$$

and so substituting these into Eq. (54), and taking the imaginary part one may write:

$$B(\omega) = \kappa + \gamma^2 \int \frac{d\nu}{2\pi} \sum_i g_i^2 \frac{F_B(\nu + \omega) - F_A(\nu)}{\left[(\nu + \omega - \epsilon_i)^2 + \gamma^2 \right] \left[(\nu + \epsilon_i)^2 + \gamma^2 \right]}. \quad (67)$$

For $B(\omega)$ to have zeros, it is necessary that the second term (which originates from pumping) should be negative, and should overcome the first term (which originates from decay). With $F_{A,B}(\nu) = \tanh[\beta(\nu \pm \mu_B/2)/2]$, it is clear that this criterion requires μ_B to be sufficiently large. As such, the following scenario describes what happens as μ_B is increased:

Very weak pumping. For large negative μ_B , one finds that $F_B(\nu + \omega) - F_A(\nu)$ is always positive, and so no zero of $B(\omega)$ exists.

Subcritical pumping. For less negative values of μ_B , there is a range of ω for which $B(\omega)$ is negative, indicating a range of gain in the spectrum. The boundary of this region, where $B(\omega) = 0$ defines an effective chemical potential μ_{eff} , but since $\mu_{\text{eff}} < \xi$ the normal state remains stable.

Critical pumping. At some value of μ_B , one finds that $\mu_{\text{eff}} = \xi$, meaning that at this value of $\omega^* = \mu_{\text{eff}} = \xi$, one has $D_{\psi^\dagger \psi}^R(\omega^*) = 0$. Hence, the gap equation first has a solution at this point, there is a real divergence of the luminescence, and the normal state is marginally stable.

Supercritical pumping. Above this critical value of μ_B , the normal state would have $\mu_{\text{eff}} > \xi$, and so would be unstable.

The actual behaviour for the polariton model of Eq. (1) is shown in Fig. 0.7; one can see that a pair of zeros of the imaginary part emerge, and then one crosses the bottom of the polariton modes. Note that in equilibrium, we have $\mu_{\text{eff}} = \mu = \mu_B$ at all conditions, and so only the last three stages of the above scenario exist; condensation occurs when the chemical potential reaches the bottom of the band. It is also important to note that the above scenario means that the Bose-Einstein distribution is not the only distribution that would allow condensation. Any distribution which has the above property, i.e. a divergence at some frequency for given values of the control parameters (density, coupling constant, etc.), is sufficient for quantum condensation in bosonic systems.

Simplified form of distribution function in high-temperature limit

The way in which the effective distribution is set by the balance of pumping and decay can be demonstrated more clearly by specialising to the case of $\gamma \ll T$, for which the pumping bath occupation functions do not change significantly across each Lorentzian broadened peak (but may vary between the two peaks). In addition, consider taking $g_i = g, \epsilon_i = \epsilon$, so that sums of

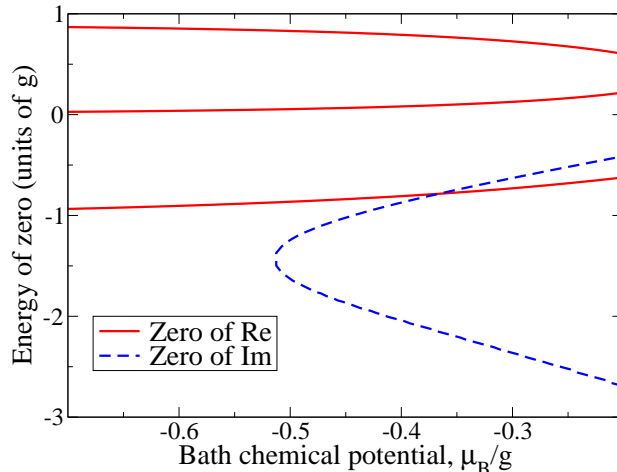


Figure 0.7: Variation of energies of zeros of real part of inverse Green's function and imaginary part as density is varied via chemical potential of pumping bath. The three solid lines correspond to (from the bottom) lower polariton, exciton, and upper polariton respectively. The point where the dashed line crosses solid line is where the condensation occurs. Adapted from Ref.[29].

two-level systems can be replaced by factors n . Then the expression in Eq. (67) can be simplified to give:

$$B(\omega) = \kappa + ng^2\gamma \frac{[F_B(\epsilon) - F_A(\epsilon - \omega)]}{(\omega - 2\epsilon)^2 + 4\gamma^2}, \quad (68)$$

where we have performed the integrals assuming the distributions are effectively constant.³ By applying the same approach to $[D_{\psi^\dagger\psi}^{-1}]^K$ one has:

$$2n_\psi(\omega) + 1 = \frac{\kappa(2n_\Psi(\omega) + 1) + \frac{ng^2\gamma}{(\omega - 2\epsilon)^2 + 4\gamma^2}[1 - F_B(\epsilon)F_A(\epsilon - \omega)]}{\kappa + \frac{ng^2\gamma}{(\omega - 2\epsilon)^2 + 4\gamma^2}[F_B(\epsilon) - F_A(\epsilon - \omega)]}. \quad (69)$$

From this expression one may first note that if $\gamma = 0$ (or more generally if $\kappa \gg g^2\gamma/[(\omega - 2\epsilon)^2 + 4\gamma^2]$), the the system distribution is the same as the distribution of the decay bath (the photons outside the cavity) and so $n_\psi(\omega) = n_\Psi(\omega)$. On the other hand, if $\kappa = 0$, (or more generally, if $\kappa \ll g^2\gamma/[(\omega - 2\epsilon)^2 + 4\gamma^2]$, which can occur near $\omega = 2\epsilon$), the distribution is set by the pumping bath. In this case, the important terms in Eq. (69) are:

$$2n_\psi(\omega) + 1 = \frac{1 - F_B(\epsilon)F_A(\epsilon - \omega)}{F_B(\epsilon) - F_A(\epsilon - \omega)} = \coth\left(\frac{\beta}{2}\left[\epsilon - \frac{\mu_B}{2} - \epsilon + \omega - \frac{\mu_B}{2}\right]\right), \quad (70)$$

which is a Bose distribution with the temperature and chemical potential of the pumping bath. Thus, the photon distribution interpolates between the decay and pumping bath, depending on the efficiency of coupling as a function of energy. An illustration of how this might look when the chemical potential of the decay bath is not too dissimilar from the pumping bath is shown in Fig. 0.8, however for realistic parameters, the chemical potential of the decay bath should be taken to $-\infty$.

³ Formally, the approximation consists of performing the contour integral, taking into account the poles at $\nu = -\omega + \epsilon_i + i\gamma$ and $\nu = -\epsilon + i\gamma$, but neglecting the poles from $F_{A,B}(\nu)$ which are at $\nu = \{-\omega + \mu_B/2, -\mu_B/2\} + i(2n + 1)\pi T$, along with neglecting $\beta\gamma$ in evaluating the residues.

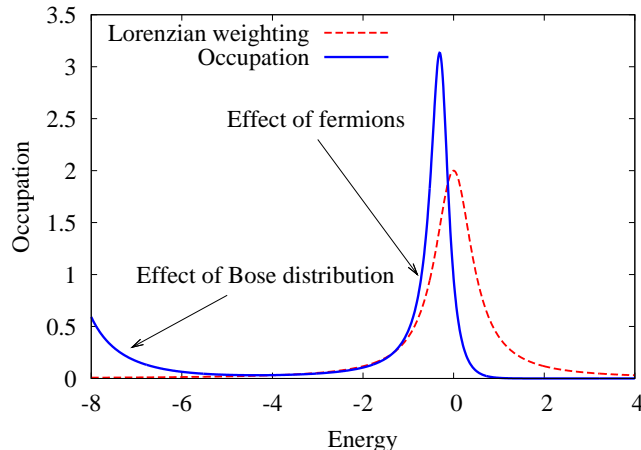


Figure 0.8: Cartoon of occupation function set by competition of bosonic bath and fermionic bath, with effect of fermionic bath moderated by a Lorentzian filter depending on excitonic energy. The chemical potential of the decay bath is at -9 , and that of the pumping bath is just below zero.

Normal-state instability for a simple laser

As for the mean-field theory, it is instructive to compare the results of Sec. 5 to those for a simple laser, in which pumping tries to fix the inversion of the gain medium, independent of frequency. The instability of the normal state can still be determined by the inverse retarded Green's function, which may in turn be found by the response of Eq. (39)–(41) to an applied force $F e^{-i\omega t}$ acting on the photons. If the force is weak, then Eq. (41) reduces to $N_i = N_0$, and taking $\lambda_{\perp} = 2\gamma$ as found previously, the equations to solve are:

$$\partial_t \psi = -i\omega_0 \psi - \kappa \psi + \sum_i g_i P_i + F e^{-i\omega t}, \quad \partial_t P_i = -2i\epsilon_i P_i - 2\gamma P_i + g_i \psi N_0, \quad (71)$$

hence writing the response as $\psi = i D_{\psi^\dagger \psi}^R(\omega) F e^{-i\omega t}$, and eliminating P_i gives:

$$[D_{\psi^\dagger \psi}^R]^{-1}(\omega) = \omega - \omega_0 + i\kappa + \sum_i \frac{g_i^2 N_0}{\omega - 2\epsilon_i + i2\gamma}. \quad (72)$$

As in the mean-field case, this same equation can be recovered from the microscopic non-equilibrium model by taking $F_{A,B}$ to be independent of frequency, and identifying $N_0 = -(F_B - F_A)/2$. The form of the inverse retarded Green's function makes much clearer the implications of this absence of frequency dependence. For the imaginary part of Eq. (72) to be zero, it is clearly necessary that $N_0 > 0$, so a region of gain can only exist when inverted.

In the special case of $\epsilon_i = \epsilon = \omega_0/2$, $g_i = g$, the zeros of the real and imaginary parts can be found explicitly to be

$$\mu_{\text{eff}} = 2\epsilon \pm \sqrt{g^2 n N_0 \frac{2\gamma}{\kappa} - 4\gamma^2}, \quad \xi = 2\epsilon, \quad 2\epsilon \pm \sqrt{-4\gamma^2 - g^2 N_0 n}, \quad (73)$$

where n is the number of two-level systems as before. From the zeros of the imaginary part, one sees that a region of gain exists only for $N_0 > 2\kappa\gamma/g^2 n$ (note that this is the laser threshold condition discussed in section 4). On the other hand, a splitting of the zeros of the real part ξ exists only if $N_0 < -4\gamma^2/g^2 n$. Thus the instability of the normal state only occurs after the normal mode splitting has collapsed. This is illustrated in Fig. 0.9. In this figure, it is also

clear that as soon as there is a region of gain, there is an instability. This is quite different from Fig. 0.7, where a region of gain, and thus zeros of the imaginary part, emerged at a lower pumping strength than was required for the instability. This meant that in the non-equilibrium condensate, a diverging distribution function exists before condensation occurs, whereas for Fig. 0.9, the distribution function has no divergence in the normal state.⁴

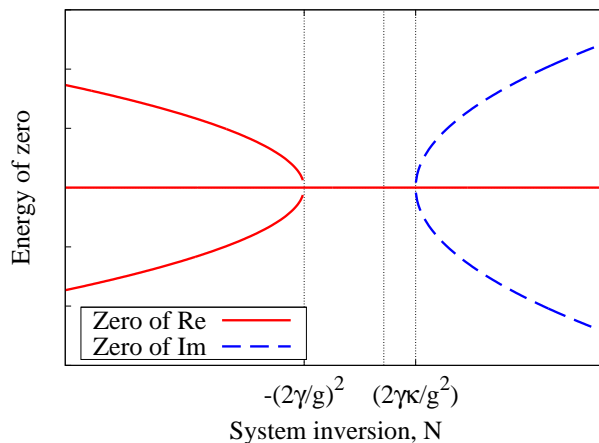


Figure 0.9: As for Fig. 0.7 but for the results of the Maxwell-Bloch equations, showing the rather different behaviour in the extreme laser limit, plotted for $\omega_0 = 2\epsilon$.

6 Fluctuations of the condensed system

When condensed, the derivation of the spectrum from the inverse Green's function written previously becomes much more involved, but the essential features of the spectrum can be determined by considering the symmetries that the system must possess — the results of this analysis are confirmed by the exact expressions for the inverse Green's functions. In particular, one may combine the Hugenholtz-Pines relation, mentioned at the end of Sec. 5, with the analytic properties of the Green's functions which imply $[D_{\psi\psi^\dagger}^R]^{-1}(\omega, p) = [D_{\psi^\dagger\psi}^R]^{-1}(-\omega, p)^*$, $[D_{\psi^\dagger\psi}^R]^{-1}(\omega, p) = [D_{\psi\psi}^R]^{-1}(-\omega, p)^*$. From these general considerations, one may find that the most general structure for sufficiently small ω, k is:

$$D_{\psi^\dagger\psi}^R(\omega, k) = \frac{C}{\det([D^R]^{-1})} = \frac{C}{\omega^2 + 2i\omega x - c^2 k^2}, \quad (74)$$

where x is an effective linewidth, and c an effective sound velocity. The form of this expression is dictated by: the need to combine symmetry under $k \rightarrow -k$; the existence of a finite linewidth; and the pole at $\omega = 0, k = 0$ that is ensured by the Hugenholtz-Pines relation. Higher order contributions could exist (and in fact do exist) for larger ω, k , but the $\omega, k \rightarrow 0$ structure is fixed by these considerations.

The above structure means that the poles of the Green's function for small k are diffusive, i.e. $\omega^* = -ix \pm i\sqrt{x^2 - c^2 k^2}$, meaning that long wavelength excitations decay, but with a lifetime

⁴If one considers the more general case with detuning, $\omega_0 \neq 2\epsilon$, a region of gain may appear before the instability occurs. Furthermore, if one also has inhomogeneous broadening, $\epsilon \neq \epsilon_j$, and different inversion for different two-level systems, a region of gain can coexist with a splitting of the normal states. However, the results for the non-equilibrium condensate shown in Fig. 0.7 had neither detuning nor inhomogeneous broadening; hence in the absence of such complications, the difference between the non-equilibrium condensate and a simple laser are particularly obvious.

that diverges for one mode as $k \rightarrow 0$. This same form is also recovered from other approaches to non-equilibrium condensates[45], including also the case of a parametrically pumped polariton system[60]. Note that if one were to naively extract a Landau critical velocity from the real part of ω^* , then this critical velocity would vanish. There has been some work on how the concept of the Landau critical velocity may be generalised for parametrically pumped condensates[61–63], however the full implications of the diffusive structure on superfluidity of incoherently pumped non-equilibrium condensates remains an open question. Because the polariton system is two-dimensional, phase fluctuations can be expected to play a particularly important role, therefore the remainder of this section will discuss how the above form of the Green's function determines the long-time correlations, and hence the lineshape, and how this connects to other approaches to deriving the polariton lineshape.

To take full account of the phase fluctuations, one must reparameterise the fluctuations as $\psi = \sqrt{\rho + \pi} e^{i\phi}$. In order that one works with fields for which there is a macroscopic expectation of $\langle \psi \rangle$ this reparameterisation must be performed in real space, and in terms of the fields on the forward and backward contours, rather than the symmetric and antisymmetric combinations of these fields. (Note that the macroscopic expectation of the anti-symmetric combination ψ_- vanishes [30].) To describe the long-time correlations, we wish to find the first order coherence function $D_{\psi^\dagger\psi}^{fb}(t) = -i\langle T_c[\psi(t, f)\psi^\dagger(0, b)] \rangle$, and corresponds to the Fourier transform of the luminescence spectrum, $\mathcal{L}(\omega)$. Since it is the phase fluctuations that dominate the long time behaviour, one may write this asymptotic behaviour in the form:

$$D_{\psi^\dagger\psi}^{fb}(t) \simeq \rho_{QC} \langle \exp[i(\phi(t) - \phi(0))] \rangle = \rho_{QC} \exp[-f(t)], \quad (75)$$

where ρ_{QC} is the quasi-condensate density. The function $f(t)$ is given by the phase-phase correlation functions, and in two dimensions is given by:

$$f(t) = i \left[D_{\phi\phi}^{fb}(t) - D_{\phi\phi}^{fb}(0) \right] = \int \frac{d\omega}{2\pi} \int \frac{kdk}{2\pi} [1 - e^{-i\omega t}] i D_{\phi\phi}^{fb}(\omega, k). \quad (76)$$

Note that expressions (75) and (76) are determined by taking the phase fluctuations to all orders. The density fluctuations give no time dependence at long times, their effect appears only in the difference between the quasi-condensate density ρ_{QC} and the total density ρ .

Since $D_{\phi\phi}^{fb}$ corresponds to the luminescence spectrum, its relation to Keldysh and retarded Green's functions is as in Eq. (62). Assuming that the condensation arises due to pumping, then as in Sec. 5, the frequency dependence near the effective chemical potential arises from the behaviour of the inverse retarded Green's function — the frequency dependence of the inverse Keldysh Green's function has no particular singularities near this point. In this case (which is also what is found from the full calculations of the microscopic theory), the singular behaviour of the $D_{\phi\phi}^{fb}$ is given by $D_{\phi\phi}^{fb} \sim |D_{\phi\phi}^R|^2$, and so:

$$f(t) = \int \frac{d\omega}{2\pi} \int \frac{kdk}{2\pi} \frac{(C^2/\rho) [1 - e^{-i\omega t}]}{|\omega^2 + 2i\omega x - c^2 k^2|^2}. \quad (77)$$

(The factor of $1/\rho$ occurs from the relation of phase-phase Green's functions to ψ, ψ^\dagger Green's functions). As one expects for a two-dimensional system, after integrating over ω , the above integral reduces to an expression $\sim \int dk/k$, and so one has logarithmic behaviour, cut off at high k by a maximum energy of excited modes, and at small k by the time dependence. At small k , the poles of the ω integral are at $\omega = \pm 2ix, \pm i(ck)^2/2x$; the first of these has a finite residue as $k \rightarrow 0$, while the latter has a residue that is diverging, and thus dominates the behaviour. The asymptotic behaviour is thus given by:

$$f(t) = \int \frac{kdk}{2\pi} \frac{C'}{4x(ck)^2} [1 - e^{-c^2 k^2 t/2x}] \quad (78)$$

(where C' is a new constant). This expression has a cutoff for small k given by $k \sim \sqrt{x/t}/c$; thus one still has power law correlations as for an equilibrium two dimensional gas, but with a different power law, now set not only by the condensate density but also by the pumping and decay strength. Were one to calculate also the long-distance correlations at equal times, one would note another difference from equilibrium. In equilibrium, the decay of long-time equal-position correlations, and long-distance equal-time correlations have the same power laws. For the spectrum in Eq. (74), the power-law for long-distance equal-time correlations is twice that of long-time equal-position decay. This is because the low momentum cutoff for long distances is always $k \sim 1/r$, whereas the long-time cutoff is $k \sim 1/ct$ in equilibrium, but $k \sim \sqrt{x/t}$ here.

Finite-size effects – lineshape of trapped system

For a confined system, the integral over k modes is replaced by a sum over a discrete set of modes; i.e.:

$$f(t) = \sum_n \int \frac{d\omega}{2\pi} \frac{C' [1 - e^{-i\omega t}]}{|\omega^2 + 2i\omega x - \xi_n^2|^2} \simeq \sum_n \frac{C'}{4x\xi_n^2} [1 - e^{-\xi_n^2 t/2x}]. \quad (79)$$

In this form, one may then consider how the value of the sum depends on the relative size of the mode spacing ΔE , the low energy cutoff $\sqrt{x/t}$, and the maximum energy E_{\max} . Let us assume the maximum energy is large, then we have a picture something like Fig. 0.10.

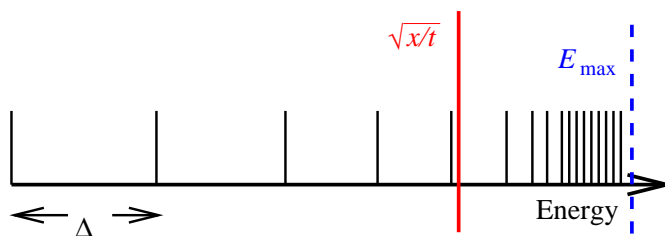


Figure 0.10: Spacing of discrete energy levels, and upper/lower cutoff energies

The sum can be divided into parts above and below the low energy cutoff, giving:

$$f(t) \simeq C' \left[\sum_{n=0}^{\xi_n < \sqrt{x/t}} \frac{t}{8x^2} + \sum_{\xi_n > \sqrt{x/t}}^{\xi_n = E_{\max}} \frac{1}{4x\xi_n^2} \right] \quad (80)$$

If both of these sums have many terms, then they may be approximated by integrals, and if the density of states $\nu(\xi)$ is $\nu_0\xi$ as it would be for a two-dimensional system with $\xi_n = cp_n$ (as illustrated in Fig. 0.10) then this becomes:

$$f(t) \simeq C' \nu_0 \left[\int_0^{\sqrt{x/t}} \frac{t}{8x^2} \xi d\xi + \int_{\sqrt{x/t}}^{E_{\max}} \frac{\xi d\xi}{4x\xi^2} \right] \simeq \frac{C' \nu_0}{16x} + \frac{C' \nu_0}{4x} \ln \left(E_{\max} \sqrt{\frac{t}{x}} \right). \quad (81)$$

What is to be noted here is that the number of terms in the first part compensates the t dependence, leading to a harmless constant. If however the number of terms in the first term is small, or is in fact truncated at its minimum value of one (which will inevitably occur for large enough t), then one instead has something of the form:

$$f(t) \simeq C' \left[\frac{t}{8x^2} + \frac{\nu_0}{4x} \ln \left(\frac{E_{\max}}{\Delta E} \right) \right], \quad (82)$$

and so one has exponential decay of coherence at long times, arising from the restricted number of modes.

If the mode spacing is such that only a single mode is involved, then Eq. (79) reduces to a single term in the sum, $\xi_0 = 0$, and the result becomes very similar to the form found from models of phase noise for a single mode condensate[64, 65], for which the lineshape interpolates between Gaussian and Lorentzian:

$$f(t) = C' \int \frac{d\omega}{2\pi} \frac{1 - e^{-i\omega t}}{(\omega^2 + 0^2)(\omega^2 + 4x^2)} = \frac{C'}{16x^2} [2xt - 1 + e^{-2xt}], \quad (83)$$

hence the decay of coherence varies from t^2 at short time (giving Gaussian lineshape at high frequencies) to t at long times (giving a Lorentzian peak at low frequencies). This result is exactly as one expects for phase noise from varying densities[65]:

$$\partial_t \phi = -iUN, \quad \partial_t N = -\Gamma N + F_\Gamma(t), \quad (84)$$

where F_Γ is a Gaussian delta correlated noise noise noise with strength P_Γ . Solving these equations in Fourier space, one has:

$$\langle |\phi_\omega|^2 \rangle = \frac{U^2}{\omega^2} \langle |N_\omega|^2 \rangle = \frac{U^2 P_\Gamma}{\omega^2(\omega^2 + \Gamma^2)}, \quad (85)$$

which is the same form as in Eq. (83)

This section thus shows another distinction between condensates and lasers in terms of many-mode or single mode fluctuations. If the system is large the spatial fluctuations resulting from the continuum of modes give rise to (in two dimensions) a power-law decay of correlations as for an infinite, equilibrium, two-dimensional quasi-condensate. For smaller systems, or at longer times, the power law crosses over to exponential decay, given by a fluctuations within the single lowest energy mode (the other modes are too high in energy to be relevant), as is characteristic for lasers.

7 Summary

This chapter has discussed in detail how the non-equilibrium Green's function formalism can be applied to study a model of microcavity polaritons, driven out of equilibrium by coupling to two baths. This model system, while not incorporating all features of the real system, allows one to make particularly transparent connections between laser theory and equilibrium descriptions, as well as allowing clear illustrations of the consequences of the approximations typically used for simple lasers. By considering steady states of the system in which there is a coherent photon field, one finds a criterion for condensation to occur, and can find a self-consistency condition which determines how the amplitude and frequency (effective chemical potential) of the coherent field depend on the strength of the pumping and decay. By considering fluctuations about steady states, one can determine whether a given steady state is stable, find the spectrum of possible excitations, and find how this spectrum is populated.

Starting from the normal state, without a condensate, and increasing pumping strength, one finds that fluctuations about the normal state become unstable at the same point that a condensed solution appears. The scenario by which this instability occurs on increasing pumping strength is quite instructive. As pumping strength increases, a region of energies for which there is gain appears in the spectrum. The energy dividing this region of gain from regions of loss defines an effective chemical potential, at which the non-equilibrium distribution function diverges. Instability occurs at a higher pumping strength, when this effective chemical potential (and thus the region of net gain) reach the normal modes of the strongly coupled system, at

which point polariton condensation occurs. Such a description unites the lasing picture of gain exceeding loss with the equilibrium picture of the chemical potential reaching the bottom of the band.

While the above description allows polariton condensation to be discussed in the language of laser theory, the results are rather different from the normal limits assumed for a simple laser theory. However, simpler laser theory results can be recovered within the model discussed here, as corresponding to a high temperature limit. In this high temperature limit, pumping corresponds to effectively white noise, and this was shown to mean that gain only exists when pumping bath is inverted. This has the consequence that in this high temperature limit, lasing and strong coupling do not coexist, whereas they can in the low temperature polariton condensate.

When considering fluctuations about the condensed state, a somewhat different distinction between simple lasers and the polariton condensate emerges: the effect of finite system size, and the spectrum of collective phase modes. For an infinite two dimensional system, the decay of coherence at long distances and long times is power law, as in equilibrium (but with different powers). For a finite system, the effects of finite lifetime and finite size combine to lead to exponential decay at long times. In the limits of very small system size, the standard result for phase noise in a single mode condensate is naturally recovered.

To summarise, the approach presented here provides a way to connect a number of different approaches to equilibrium and non-equilibrium condensates, as well as theories of lasers, in a transparent manner, allowing one to understand the significance of various approximations, as well as the relations between some of the other approaches one may use.

Bibliography

- [1] J. Kasprzak, M. Richard, S. Kundermann, A. Baas, P. Jeambrun, J. M. J. Keeling, F. M. Marchetti, M. H. Szymańska, R. André, J. L. Staehli, et al., *Nature* **443**, 409 (2006).
- [2] S. O. Demokritov, V. E. Demidov, O. Dzyapko, G. A. Melkov, A. A. Serga, B. Hillebrands, and A. N. Slavin, *Nature* **443**, 430 (2006).
- [3] J. P. Eisenstein and A. H. MacDonald, *Nature* **432**, 691 (2004).
- [4] C. Rüegg, N. Cavadinin, A. Furrer, H.-U. Güdel, K. Krämer, H. Mukta, A. Wildes, K. Habicht, and P. Worderswisch, *Nature* **423**, 62 (2003).
- [5] L. V. Butov, C. W. Lai, A. L. Ivanov, A. C. Gossard, and D. S. Chemla, *Nature* **417**, 47 (2002).
- [6] L. V. Butov, A. C. Gossard, and D. S. Chemla, *Nature* **418**, 751 (2002).
- [7] D. Snoke, S. Denev, Y. Liu, L. Pfeiffer, and K. West, *Nature* **418**, 754 (2002).
- [8] E. W. Streed, A. P. Chikkatur, T. L. Gustavson, M. Boyd, Y. Torii, D. Schneble, G. K. Campbell, D. E. Pritchard, and W. Ketterle, *Rev. Sci. Instrum.* **77**, 023106 (2006).
- [9] A. T. Hammack, L. V. Butov, L. Mouchliadis, A. L. Ivanov, and A. C. Gossard, *Phys. Rev. B* **76**, 193308 (2007).
- [10] H. Deng, D. Press, S. Götzinger, G. S. Solomon, R. Hey, K. H. Ploog, and Y. Yamamoto, *Phys. Rev. Lett.* **97**, 146402 (2006).
- [11] M. S. Skolnick, T. A. Fisher, and D. M. Whittaker, *Semicond. Sci. Technol.* **13**, 645 (1998).
- [12] V. Savona, C. Piermarocchi, A. Quattropani, P. Schwendimann, and F. Tassone, *Phase Transitions* **68**, 169 (1999).
- [13] Y. Yamamoto, F. Tassone, and H. Cao, *Semiconductor Cavity Quantum Electrodynamics*, vol. 167 of *Springer Tracts in Modern Physics* (Springer-Verlag, Berlin, 2000).
- [14] C. Ciuti, P. Schwendimann, and A. Quattropani, *Semicond. Sci. Technol.* **18**, S279 (2003).
- [15] B. Deveaud, ed., *Special Issue: Physics of Semiconductor Microcavities*, vol. 242 of *Phys. Stat. Sol. (b)* (2005).
- [16] J. Keeling, F. M. Marchetti, M. H. Szymańska, and P. B. Littlewood, *Semicond. Sci. Technol.* **22**, R1 (2007).
- [17] A. V. Kavokin, J. J. Baumberg, G. Malpuech, and F. P. Laussy, *Microcavities* (Oxford University Press, Oxford, 2007).

- [18] H. Cao, *J. Phys. A: Math. Gen.* **38**, 10497 (2005).
- [19] H. E. Türeci, L. Ge, S. Rotter, and A. D. Stone, *Science* **320**, 643 (2008).
- [20] M.-O. Mewes, M. R. Andrews, D. M. Kurn, D. S. Durfee, C. G. Townsend, and W. Ketterle, *Phys. Rev. Lett.* **78**, 582 (1997).
- [21] I. Bloch, T. W. Hänsch, and T. Esslinger, *Phys. Rev. Lett.* **82**, 3008 (1999).
- [22] E. W. Hagley, L. Deng, M. Kozuma, J. Wen, S. L. Rolston, and W. D. Phillips, *Science* **283**, 1706 (1999).
- [23] M. H. Szymanska and P. B. Littlewood, *Solid State Commun.* **124**, 103 (2002).
- [24] M. H. Szymanska, P. B. Littlewood, and B. D. Simons, *Phys. Rev. A* **68**, 013818 (2003).
- [25] A. A. Abrikosov and L. P. Gor'kov, *Sov. Phys. JETP* **12**, 1243 (1960).
- [26] P. W. Anderson, *J. Phys. Chem. Solids* **11**, 26 (1959).
- [27] F. M. Marchetti, B. D. Simons, and P. B. Littlewood, *Phys. Rev. B* **70**, 155327 (2004).
- [28] M. H. Szymańska, J. Keeling, and P. B. Littlewood, *Phys. Rev. Lett.* **96**, 230602 (2006).
- [29] M. H. Szymańska, J. Keeling, and P. B. Littlewood, *Phys. Rev. B* **75**, 195331 (2007).
- [30] A. Kamenev, in *Nanophysics: Coherence and transport*, edited by H. Bouchiat, Y. Gefen, S. Guéron, G. Montambaux, and J. Dalibard (Elsevier, Amsterdam, 2005), vol. LXXXI of *Les Houches*, p. 177.
- [31] L. V. Keldysh, *JETP* **20**, 1018 (1965).
- [32] P. Danielewicz, *Ann. Phys.* **152**, 239 (1984).
- [33] E. M. Lifshitz and L. P. Pitaevskii, *Physical Kinetics*, vol. 10 of *Course of theoretical Physics* (Butterworth-Heinemann, Oxford, 1981).
- [34] F. Tassone, C. Piermarocchi, V. Savona, A. Quattropani, and P. Schwendimann, *Phys. Rev. B* **56**, 7554 (1997).
- [35] F. Tassone and Y. Yamamoto, *Phys. Rev. B* **59**, 10830 (1999).
- [36] G. Malpuech, A. Di Carlo, A. Kavokin, J. J. Baumberg, M. Zamfirescu, and P. Lugli, *Appl. Phys. Lett.* **81**, 412 (2002).
- [37] G. Malpuech, A. Kavokin, A. Di Carlo, and J. J. Baumberg, *Phys. Rev. B* **65**, 153310 (2002).
- [38] D. Porras, C. Ciuti, J. J. Baumberg, and C. Tejedor, *Phys. Rev. B* **66**, 085304 (2002).
- [39] T. D. Doan, H. T. Cao, D. B. Tran Thoai, and H. Haug, *Phys. Rev. B* **72**, 085301 (2005).
- [40] T. D. Doan, H. T. Cao, D. B. Tran Thoai, and H. Haug, *Phys. Rev. B* **74**, 115316 (2006).
- [41] T. D. Doan, H. T. Cao, D. B. Tran Thoai, and H. Haug, *Phys. Rev. B* **78**, 205306 (2008).
- [42] B. Mieck and H. Haug, *Phys. Rev. B* **66**, 075111 (2002).
- [43] I. Carusotto and C. Ciuti, *Phys. Rev. B* **72**, 125335 (2005).

- [44] M. Wouters and V. Savona, *Phys. Rev. B* **79**, 165302 (2009).
- [45] M. Wouters and I. Carusotto, *Phys. Rev. Lett.* **99**, 140402 (2007).
- [46] M. Wouters, I. Carusotto, and C. Ciuti, *Phys. Rev. B* **77**, 115340 (2008).
- [47] J. Keeling and N. G. Berloff, *Phys. Rev. Lett.* **100**, 250401 (2008).
- [48] L. Kadanoff and G. Baym, *Quantum Statistical Mechanics* (W. A. Benjamin, New York, 1962).
- [49] M. O. Scully and M. S. Zubairy, *Quantum Optics* (Cambridge University Press, 1997).
- [50] G. W. Ford and R. F. O'Connell, *Phys. Rev. Lett.* **77**, 798 (1996).
- [51] P. R. Eastham and P. B. Littlewood, *Solid State Commun.* **116**, 357 (2000).
- [52] J. Keeling, P. R. Eastham, M. H. Szymanska, and P. B. Littlewood, *Phys. Rev. Lett.* **93**, 226403 (2004).
- [53] F. M. Marchetti, J. Keeling, M. H. Szymańska, and P. B. Littlewood, *Phys. Rev. Lett.* (2006).
- [54] E. M. Lifshitz and L. P. Pitaevskii, *Statistical Physics, Part II*, vol. 5 of *Course of theoretical Physics* (Butterworth-Heinemann, Oxford, 1980).
- [55] A. Abrikosov, L. Gorkov, and I. Dzyaloshinski, *Methods of Quantum Field Theory in Statistical Physics* (Dover, New York, 1975).
- [56] M. Randeria, in *Bose-Einstein Condensation*, edited by A. Griffin, D. Snoke, and S. Stringari (Cambridge University Press, Cambridge, 1995), p. 355.
- [57] M. H. Szymańska, Ph.D. thesis, University of Cambridge (2002), arXiv:cond-mat/0204294.
- [58] N. M. Hugenholtz and D. Pines, *Phys. Rev.* **116**, 489 (1959).
- [59] V. N. Popov, *Functional Integrals in Quantum Field Theory and Statistical Physics* (D. Reidel, Dordrecht, 1983).
- [60] M. Wouters and I. Carusotto, *Phys. Rev. A* **76**, 043807 (2007).
- [61] I. Carusotto and C. Ciuti, *Phys. Rev. Lett.* **93**, 166401 (2004).
- [62] C. Ciuti and I. Carusotto, *Phys. Stat. Sol. (b)* **242**, 2224 (2005).
- [63] A. Amo, J. Lefrère, S. Pigeon, C. Adrados, C. Ciuti, I. Carusotto, R. Houdré, E. Giacobino, and A. Bramati, *Nature Phys.* **5**, 805 (2009).
- [64] D. M. Whittaker and P. R. Eastham, *EPL (Europhysics Letters)* **87**, 27002 (2009).
- [65] R. Kubo, *J. Phys. Soc. Jap* **9**, 935 (1954).